ERDC/CRREL TR-00-18

Cold Regions Research and Engineering Laboratory

US Army Corps of Engineers®
Engineer Research and Development Center

# Geological Investigations and Hydrogeological Model of Fort Richardson, Alaska

Lewis E. Hunter, Daniel E. Lawson, Susan R. Bigl,
Beth N. Astley, Colby F. Snyder, and Frank E. Perron, Jr.

September 2000

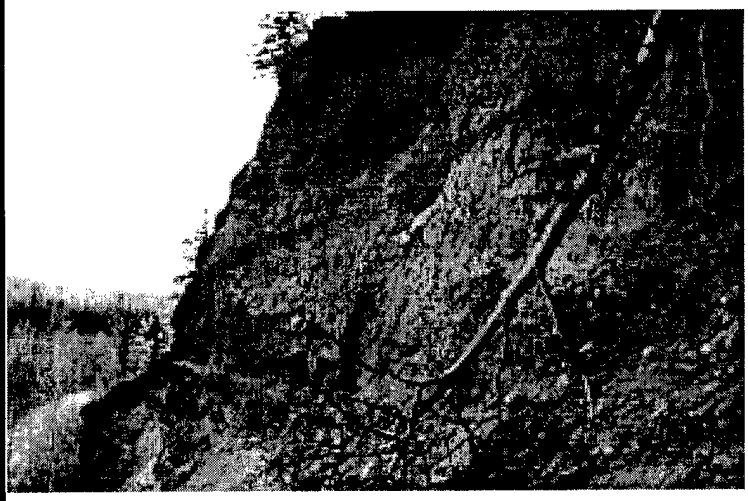

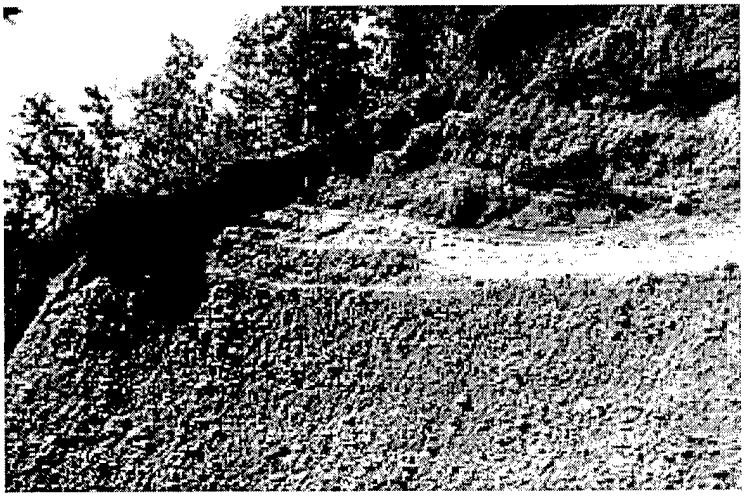

**Abstract:** The glacial stratigraphy of Fort Richardson reflects deposition in glacial and glacial–marine environments during multiple retreat phases following the last glacial maximum. A preliminary model relied heavily on the glacial history of the region, mapping by the U.S. Geological Survey, and limited borehole logs. This report expands on that model and describes new subsurface data obtained from field observations and descriptions of stratigraphic exposures and core samples from 28 new boreholes between 1997 and 1998. Geophysical techniques were applied to seven of the new boreholes and 25 existing monitoring wells, augmenting surface techniques (ground resistivity and ground penetrating radar). Beneath the cantonment is a thick unconfined aquifer, apparently deposited as a large alluvial fan (Mountain View fan), that overlies a fine-grained confining layer composed of mud and diamicton. The diamicton is a subglacial lodgement deposit bracketed by stratified debris flow deposits, being thickest to the southeast, dipping and thinning to the north and west where deposits of the Mountain View fan truncate the confining horizon, providing potential hydraulic communication between the upper (unconfined) and lower (confined) aquifers. A second mud–diamicton horizon forms a deeper (38–66 m depth) confining layer and also appears to extend across the cantonment. Between the upper and lower confining diamicton horizons are coarse, sandy gravels that make up a confined aquifer. Ground water in the unconfined aquifer flows generally to the northwest, presumably recharged by Ship Creek. When ground water levels are low (i.e., winter), flow is locally diverted by irregularities in the surface of the upper confining layer. When recharge is high, regional flow is unaffected by these irregularities. Ground water in the confined aquifer also flows to the northwest, following the slope of the potentiometric surface.

**How to get copies of CRREL technical publications:**

Department of Defense personnel and contractors may order reports through the Defense Technical Information Center:

DTIC-BR SUITE 0944
8725 JOHN J KINGMAN RD
FT BELVOIR VA 22060-6218
Telephone (800) 225-3842
E-mail help@dtic.mil
msorders@dtic.mil
WWW http://www.dtic.mil/

All others may order reports through the National Technical Information Service:

NTIS
5285 PORT ROYAL RD
SPRINGFIELD VA 22161
Telephone (703) 487-4650
(703) 487-4639 (TDD for the hearing-impaired)
E-mail orders@ntis.fedworld.gov
WWW http://www.ntis.gov/index.html

A complete list of all CRREL technical publications is available from

USACRREL (CEERD-IM-HL)
72 LYME RD
HANOVER NH 03755-1290
Telephone (603) 646-4338
E-mail erhoff@crrel.usace.army.mil

**For information on all aspects of the Cold Regions Research and Engineering Laboratory, visit our World Wide Web site:**

http://www.crrel.usace.army.mil

Technical Report
ERDC/CRREL TR-00-18

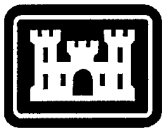

US Army Corps
of Engineers®
Cold Regions Research &
Engineering Laboratory

# Geological Investigations and Hydrogeological Model of Fort Richardson, Alaska

Lewis E. Hunter, Daniel E. Lawson, Susan R. Bigl,
Beth N. Astley, Colby F. Snyder, and Frank E. Perron, Jr.

September 2000

Prepared for
OFFICE OF THE CHIEF OF ENGINEERS

## PREFACE

This report was prepared by Dr. Lewis E. Hunter, Research Physical Scientist, Dr. Daniel E. Lawson, Research Physical Scientist, Susan R. Bigl, Research Physical Scientist, Beth N. Astley, Research Physical Scientist, Colby F. Snyder, Research Physical Scientist, Geochemical Sciences Division, and Frank E. Perron, Jr., Engineering Technician, Geophysical Sciences Division, U.S. Army Engineer Research and Development Center, Cold Regions Research and Engineering Laboratory (CRREL), Hanover, N.H.

Funding and support for this research was provided by the U.S. Army Alaska, Environmental Resources Department, Directorate of Public Works, Fort Richardson, Alaska. Technical review was provided by Dr. Steven Arcone and Charles Collins, both of CRREL.

The authors thank Henry Schmoll and Lynn Yehle of USGS for numerous discussions and comments on the text.

## CONTENTS



## ILLUSTRATIONS

Figure

## TABLES

Table

## EXECUTIVE SUMMARY

The glacial stratigraphy of Fort Richardson reflects deposition in glacial and glacial–marine environments during multiple retreat phases following the last glacial maximum. A preliminary model by Hunter et al. (1997c) relied heavily on the glacial history of the region, mapping by the U.S. Geological Survey, and limited borehole logs. This report expands on that preliminary model and describes new subsurface data.

Geological information has been collected from field observations and descriptions of stratigraphic exposures and core samples collected while drilling 28 new boreholes between 1997 and 1998. In November 1998, downhole geophysical techniques were applied to seven of the new boreholes and 25 existing monitoring wells. These surveys augment surface geophysical techniques, including ground resistivity and ground penetrating radar. Stratigraphic analyses have been combined with geologic interpretations of the boreholes, cross correlation of the geophysical logs, and results of geophysical surveys to define conditions below Fort Richardson.

The hydrogeology beneath the cantonment area is characterized by a thick unconfined aquifer, apparently deposited as a large alluvial fan (Mountain View fan). This sand and gravel unit approaches 50 m in thickness on the north side of the cantonment near the Elmendorf Moraine and overlies a fine-grained confining layer composed of mud and diamicton below the main cantonment. The mud forms a pebble-rich horizon containing outsized clasts (i.e., dropstones) deposited in the vicinity of a calving glacier margin. The mud is of variable thickness and forms a drape deposit over the diamicton. This mud is transitional with sand at higher elevations where shallow water conditions or proximity to a sediment source are indicated. We interpret the diamicton as a subglacial lodgement deposit (generally unstructured diamicton) bracketed by stratified debris flow deposits (stratified diamicton). The diamicton is thickest to the southeast; it dips and thins to the north and west where deposits of the Mountain View fan appear to truncate the confining horizon, providing potential hydraulic communication between the upper (unconfined) and lower (confined) aquifers.

A second mud-diamicton horizon forms a deeper (38–66 m depth) confining layer and also appears to extend across the cantonment area; however, insufficient borehole coverage makes stratigraphic correlation difficult. Between the upper and lower confining diamicton horizons are coarse, sandy gravels that make up a confined aquifer.

Ground water in the unconfined aquifer flows generally to the northwest, presumably recharged by Ship Creek. When ground water levels are low (i.e., in the winter), flow is locally diverted by irregularities in the surface of the upper confining layer. When recharge is high, regional flow is unaffected by these irregularities. Ground water in the confined aquifer also flows to the northwest, following the slope of the potentiometric surface. The upper unconfined and lower confined aquifers appear to merge below the northern area of the cantonment where the confining layer is absent.

# Geological Investigations and Hydrogeological Model of Fort Richardson, Alaska

LEWIS E. HUNTER, DANIEL E. LAWSON, SUSAN R. BIGL,
BETH N. ASTLEY, COLBY F. SNYDER, AND FRANK E. PERRON, JR.

## INTRODUCTION

Fort Richardson is a 251-km$^2$ Army installation located in the Municipality of Anchorage, Alaska (Fig. 1). Built to defend Alaska against foreign invasion, recent military activities include cold weather, mountain warfare, and rapid deployment training. Because site activities included the use of several potential environmental contaminants, the Department of Defense began an Installation Restoration Program to investigate known or suspected contaminant sources (USACE 1997a–c). In June 1994, Fort Richardson was added to the United States Environmental Protection Agency's National Priority List. Site investigations found various levels of contaminated soil and ground water; several contaminants with widely varying concentrations were found in the immediate area of the cantonment (Table 1).

In 1995, the Cold Regions Research and Engineering Laboratory (CRREL) began site investigations to characterize subsurface conditions influencing ground water and contaminant transport. As a result, a variety of lithologic and geophysical data have been collected and a conceptual stratigraphic model was proposed by Hunter et al. (1997a) that was based on available geologic and hydrologic data, and analyses of river cuts, gravel pits, and shallow excavations. Additionally, ground-penetrating radar (Strasser et al. 1996) and DC resistivity (Hunter et al. 1997b) were evaluated as nonintrusive ways to investigate subsurface conditions. In 1998, a drilling program was started to further investigate the subsurface conditions and address data gaps identified by Hunter et al. (1997a). As part of this program, soil samples were collected and described, and 32 wells were logged using downhole geophysical techniques. The objective of this report is to evaluate these new data and to modify the conceptual stratigraphic model to provide a better understanding of the subsurface conditions controlling ground water and contaminant transport.

### Geological setting

The geology of Fort Richardson and adjacent lands is characterized by glacial, glacial–marine (glacioestuarine), and glacioalluvial deposits of Quaternary age (Fig. 2; Miller and Dobrovolny 1959; Cederstrom et al. 1964; Schmoll and Dobrovolny 1972; Yehle and Schmoll 1987a, b, 1989; Yehle et al. 1990, 1992; Schmoll et al. 1996). These deposits thicken westward from the base of the Chugach Mountains. Underlying the Fort Richardson cantonment, glacial sediments range from 70 to 98 m thick, according to well logs (Cederstrom et al. 1964) and recent logging of monitoring well AP-3905 (Fig. 3a; Hunter et al. 1999), but reach up to 213 m elsewhere in the Anchorage basin.*

A large alluvial fan (Mountain View fan) emanating from the Eagle River Valley extends under the Fort Richardson cantonment (Fig. 1 and 2). Sloping gently to the west–southwest, the fan extends beneath parts of Elmendorf Air Force Base and downtown Anchorage, and is truncated to the west by sea bluffs along Knik Arm. Composed of stratified outwash, the fan was likely deposited by ice-marginal, glacially fed streams, primarily during outburst-flooding events from ice-dammed lakes in the Eagle River Valley (Schmoll et al. 1996). The fan is bordered on the north by the Elmendorf Moraine, which forms a low-relief ridge trending west to east from Knik Arm to the mouth of the Eagle River Valley.

Near the southern margin of the fan, several low hills protrude through younger glacial sediment (Hunter et

*Personal communication with H.R. Schmoll, USGS, 1999.


**Figure 1. Location of Fort Richardson relative to Anchorage, Alaska (outline delineates boundary of fort).**

**Table 1. Identified or suspected contaminants, Fort Richardson, Alaska.**

| *Operable unit* | *Source area* | *Contaminants** |
|---|---|---|
| A | Building 986 Petroleum, Oil and Lubricant Laboratory Dry Well | POLs, solvents, semi-volatile organics, and metals. |
| | Roosevelt Road Transmitter Site Leachfield | PCBs, solvents, and metals. |
| | Ruff Road Fire Training Area | POLs and dioxins. |
| B | Poleline Road Disposal Area | VOCs, chemical warefare materials. |
| C | Eagle River Flats | White phosphorus. |
| D | Building 35-752 | PCBs, diesel, alcohols, paint waste, petroleum hydrocarbons, and dry-cleaning solvents. |
| | Building 700/718 | PCBs, POLs, solvents, mineral spirits, alcohols, ethylene glycol, Stoddard solvent, MEK, cyclohexylamine, PCE, and TCE. |
| | Building 704 | POLs, chlorinated solvents, alcohols, mineral spirits, paint waste, and ballast water. |
| | Building 726 | PCE, TCE, Stoddard solvent and other chlorinated solvents. |
| | Building 796 | Battery acid and lead. |
| | Building 955 | PCBs, petroleum hydrocarbons, VOCs, semi-VOCs, ethlyene glycol, metals, and pesticides. |
| | Building 45-590 | Petroleum hydrocarbons and PCE. |
| | Dust Palliative Areas | PCBs, petroleum hydrocarbons, and metals. |
| | Landfill Former Fire Training Area | POLs and VOCs. |
| | Landfill Grease Pits | POLs, solvents, ethylene glycol, paint waste, and pesticides. |
| | Stormwater Drainage Outfall to Ship Creek | Any hazardous substance used at Fort Richardson. |

*MEK— methyl ethyl ketone; PCBs—polychlorinalted biphenyls; PCE—tetrachloroethylene; POLs—petroleum, oil, and lubricants; TCE—trichloroethene; VOCs—volatile organic compounds.

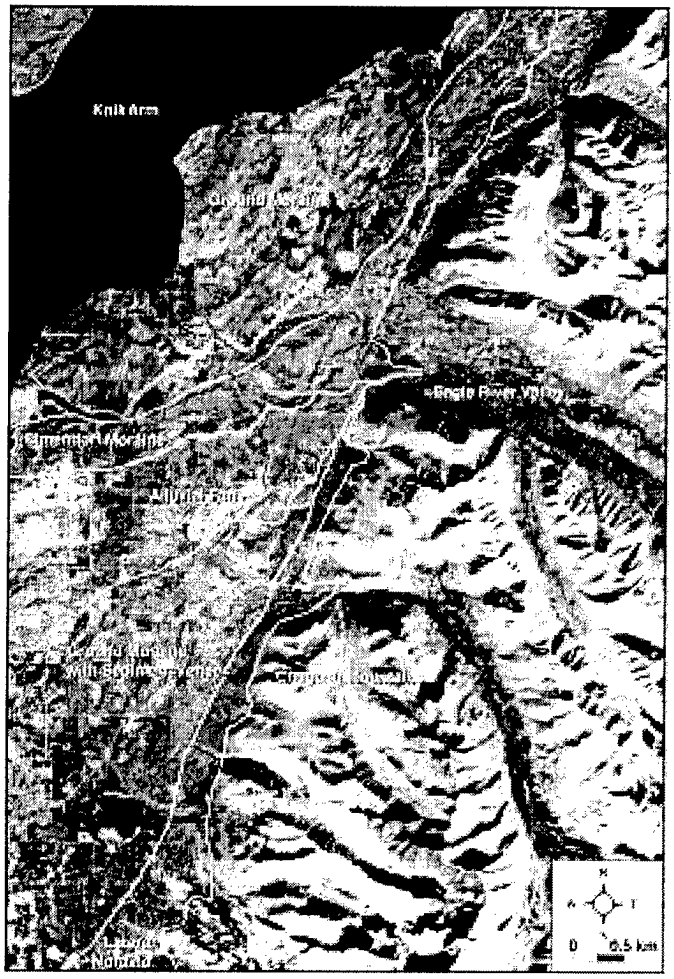


**Figure 2. General geological setting of Fort Richardson in the Anchorage Lowland.**

al. 2000). These hills are streamlined and composed of ground moraine (glacial diamicton) that appears to extend underneath the alluvial fan and fine-grained silt deposits. These silty deposits may correlate with upper sections of the Bootlegger Cove silt (e.g., Miller and Dobrovolny 1959, Reger et al. 1995, Schmoll et al. 1996); however, laterally continuous stratigraphic data are unavailable to confirm this interpretation.

## Glacial history

Schmoll et al. (1996) and Yehle et al. (1992) concluded that multiple advance and retreat phases associated with the last glaciation (Late Wisconsinan) deposited the sediments that cover bedrock in the Anchorage lowland. We only briefly summarize the glacial history in this section; a more detailed description is given by Hunter et al. (2000).

About 20,000 years ago, glaciers flowed out of the Alaska Range and the Chugach and Talkeetna Mountains, coalescing in Cook Inlet and the Susitna Lowland. Glacier ice filled Knik Arm and overtopped ridges along the Chugach Mountains.

The retreat of this large ice mass from Cook Inlet probably began around 18,000 to 20,000 $^{14}C$ years ago and was accompanied by a marine transgression over the isostatically depressed basin. During this period, glacial-marine sediments were deposited over subglacial diamictons (ground moraine) and outwash gravels that were deposited during the preceding glaciation. Several fluctuations in the position of the ice sheet terminus were accompanied by marine inundations of the Rabbit Creek and the South Fork of Campbell Creek areas.

A larger retreat to the north of unknown distance followed, with a marine incursion depositing the lowermost sections of the Bootlegger Cove Formation. Subsequently, ice readvanced into the Anchorage basin, depositing the Dishno Pond moraines along the Chugach Mountains and an age-equivalent ground moraine on top of the Bootlegger Cove Formation in

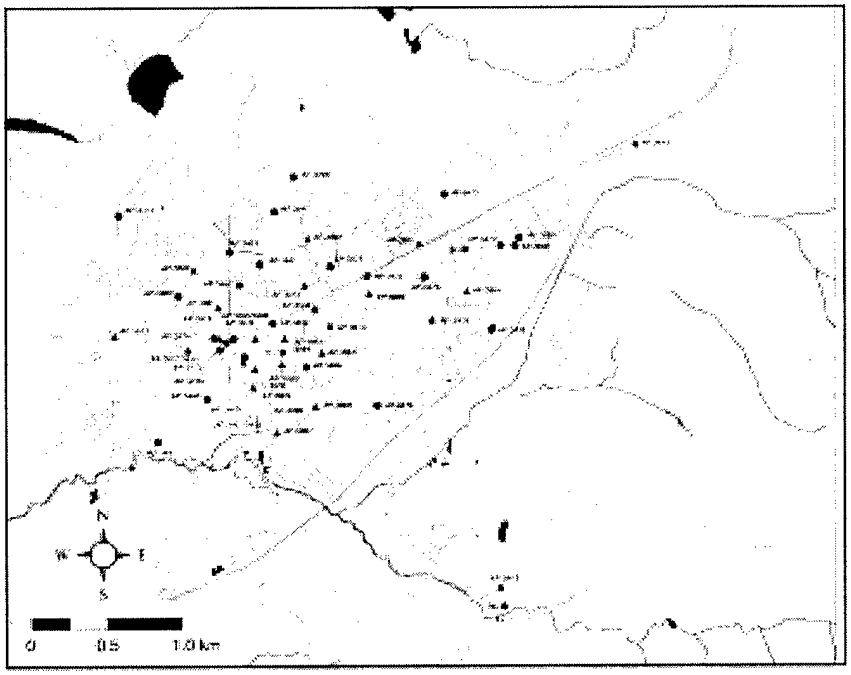


a. Boreholes and monitoring wells.

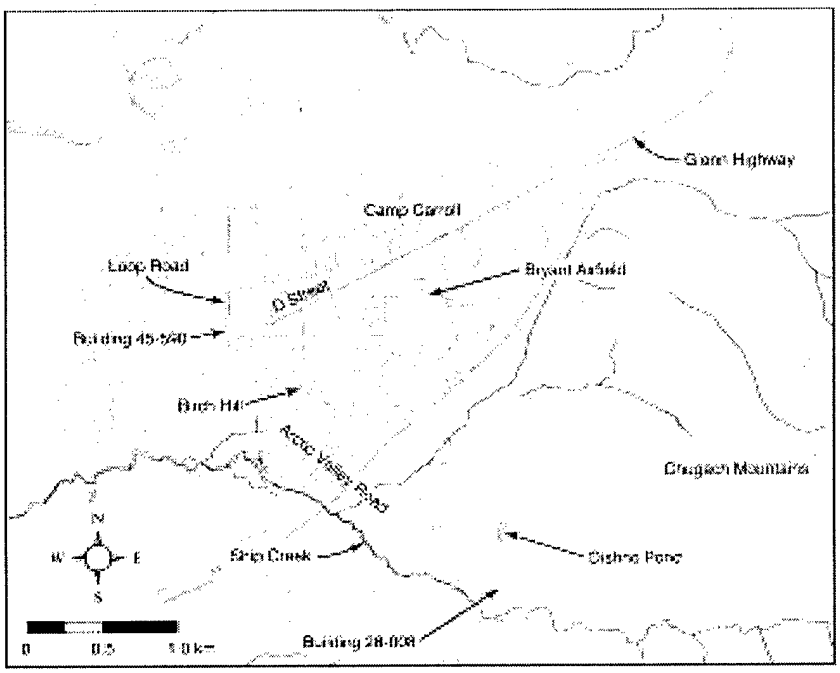


b. Features and areas.

**Figure 3. Locations of selected wells, features, and areas.**

the Fort Richardson area (Schmoll et al. 1996, Hunter et al. 2000). Marine conditions and sedimentation continued in the Campbell and Chester Creek areas during this advance phase (Fig. 1).

The progressive recession of glaciers up lower Knik Arm deposited ice-rafted debris in the lower Bootlegger Cove Formation around 14,900 ± 350 $^{14}C$ years B.P. (Schmoll et al. 1972, Reger et al. 1995). Although the extent of this recession is not known, silt deposits equivalent to the Bootlegger Cove Formation extend about 60 km up the Susitna Valley (Reger et al. 1995). During this retreat phase, the Fort Richardson area was submerged about 140 m below sea level. Wave action and coastal erosion along the base of the Chugach

Mountains stripped away some of the older sediments, including Fort Richardson age and older lateral moraines (Schmoll et al. 1996).

Glacier ice returned to Knik Arm during the Elmendorf readvance, around 13,500–14,000 $^{14}C$ years ago (Reger et al. 1995). Sand layers and a general coarsening in the upper section of the Bootlegger Cove Formation indicate encroachment of the advancing glacier into the Anchorage basin (Miller and Dobrovolny 1959, Karlstrom 1964, Yehle et al. 1986). Construction of the Elmendorf Moraine around 13,500 $^{14}C$ years ago records the end of this readvance (Reger et al. 1995).

Schmoll et al. (1996) suggest that the Mountain View fan was formed shortly thereafter by multiple catastrophic drainages of ice- or moraine-dammed lakes in the Eagle River Valley. These floods were the precursor to the final retreat of ice from the Anchorage region. Morainal and alluvial deposits were probably eroded during each catastrophic drainage of these lakes. An understanding of such erosional events is important to interpreting the subsurface stratigraphy, as they produce gaps in the vertical sequence. In addition, this erosion affects the lateral extent of both fine-grained confining layers and coarse-grained aquifer-bearing horizons.

Subsequently, rapid retreat of Elmendorf ice appears to have formed the hummocky topography in the Susitna Valley and upper Knik Arm, as isolated masses of ice left behind during the retreat melted. Streams such as the Eagle River and Ship Creek also incised themselves into their ancestral channels as the ice margin receded and isostatic rebound lifted the area. Reger et al. (1995) suggest that the ice margin had retreated to the Palmer area by around 9000 $^{14}C$ years B.P., about the same time as ice retreated to the Turnagain Pass area at the head of Turnagain Arm.

## Previous work

Hydrological and geological data were acquired through a detailed literature search of studies conducted in the Fort Richardson and Anchorage areas (Hunter et al. 1997b, 2000). Using these data, we developed our preliminary conceptual model of the surficial geology and subsurface stratigraphy of the Fort Richardson cantonment area (Hunter et al. 2000).

Subsequently, we have conducted geophysical surveys using ground-penetrating radar (GPR) and DC resistivity soundings to test and refine this model. The GPR studies yielded limited data because of shallow depths of penetration (less than 20 m). We think this results from radiowave attenuation in the silt and scattering losses from the wide size distribution (or texture) of the near-surface gravels, which are common across the area (Strasser et al. 1996, Hunter et al. 2000). Figure 4 is an example of a GPR profile obtained along Arctic Valley Road. The profile shows a strong reflector at 5 to 10 m depth, which we interpreted to be the contact between diamicton and overlying sand and gravel of the Mountain View fan. We interpret the lens-shaped reflector as a cut-and-fill sequence produced by channel migration, incision, and infilling while the fan formed. The intermittent reflector at 12 to 18 m depth appears to correspond with the surface of a silty diamicton that Cederstrom et al. (1964) observed in a nearby borehole, and which we encountered in AP-3887 (Fig. 3a).

Reconnaissance ground resistivity surveys subsequently revealed a horizon with low resistivity (100 to 250 Ω-m) that corresponds with the shallow reflector seen in a few of the GPR profiles (Strasser et al. 1996,

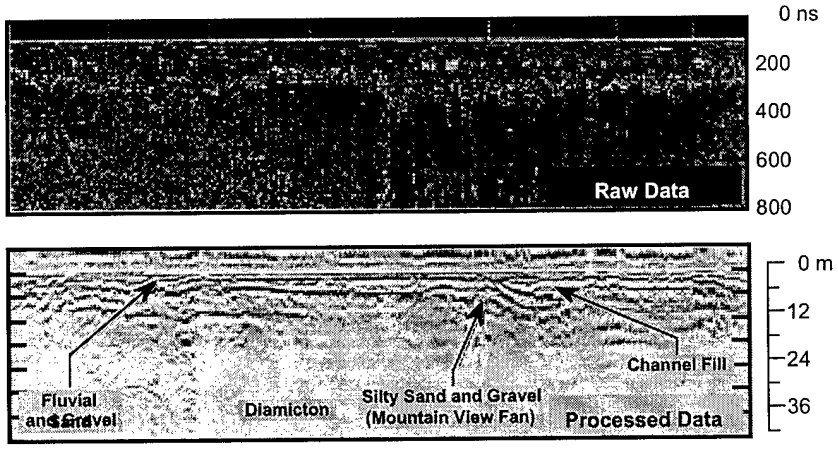


**Figure 4. 50-Mhz radar profile collected along Arctic Valley Road showing a shallow, gently dipping reflector at the base of the Mountain View fan.**

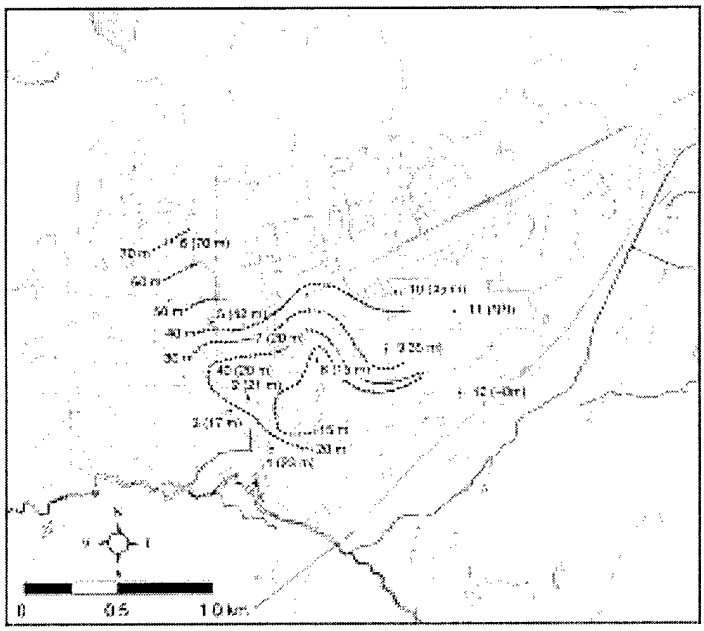


**Figure 5. Preliminary map showing the depth to the confining layer, based on surface resistivity data. (From Hunter et al. 1997b.)**

Hunter et al. 2000). The relatively conductive, fine-grained diamicton or glacial-marine mud forms the base of the seasonal, upper aquifer (Fig. 5). Similarly, it is a confining layer for a lower aquifer that exists beneath much of the cantonment area. Resistivity data, however, show that this confining layer probably dips to the north and west in the northern and western parts of the cantonment and may locally be absent.

Successful GPR surveys have also been obtained in the vicinity of Building 28-008, where two strong reflectors were identified (Astley et al. 1999) (Fig. 3). The upper reflector was generally at 14 to 18.5 m depth, and we interpreted it as the water table. A second reflector at 21 to 23 m depth corresponds with the top of a dense, fine-grained diamicton that acts as a confining layer. Ground resistivity studies here also consistently detected the fine-grained diamicton at a similar depth. This layer is assumed to be equivalent to the Dishno Pond ground moraine (Schmoll et al. 1996; Yehle et al. 1990; Yehle and Schmoll 1987a, 1989).

## CURRENT INVESTIGATIONS

Our current focus is the stratigraphy of the shallow subsurface materials, defining the sedimentary architecture, and the spatial distribution of potential confining layers and ground water aquifers. We examined outcrops, interpreted borehole logs and samples, and conducted geophysical surveys of boreholes. We have correlated the results with those obtained previously on near-surface materials.

### Outcrop analyses

We analyzed outcrops along Ship Creek, within a gravel pit near Bryant Air Field, and in a foxhole dug for training exercises between AP-3892 and AP-3894 (Fig. 3). We described the sedimentary contacts and characteristics, including the vertical and lateral changes in sediment type, texture, and structure.

### Borehole analyses

We observed the sedimentary characteristics of near-surface materials in borehole samples collected during the drilling of monitoring wells between summer 1997 and spring 1998. Ambler Exploration drilled 28 boreholes using an air rotary drill rig (Table 2; Fig. 3a and 6). Soil samples up to 46 cm long were collected at 1.5- and 3-m intervals using a 5-cm wide split-spoon sampler (Fig. 7). Personnel from the U.S. Army Engineer District, Alaska, classified these samples following ASTM (1995) standards, while CRREL personnel interpreted their geologic properties (Hunter et al. 1999). In addition, we reinterpreted the sediment types and

**Table 2. Wells analyzed to evaluate Fort Richardson cantonment subsurface geology.**

| *ID number* | *Field ID* | *Northing* | *Easting* | *Depth (m)* | *Elevation (m)* | *Logged** |
|---|---|---|---|---|---|---|
| | | | **a. Existing wells.** | | | |
| AP-3220 | MW-8 | 124406 | 129156 | 73.8 | 124.4 | x |
| AP-3375 | AP3375 | 120423 | 130810 | 49.6 | 100.0 | x |
| AP-3461 | AP-T2 | 120541 | 127682 | 43.1 | 92.5 | x |
| AP-3462 | AP-T3 | 119643 | 126751 | 40.1 | 90.4 | x |
| AP-3463 | AP-T4 | 121082 | 126333 | 41.1 | 90.6 | x |
| AP-3469 | AP-6 | 116539 | 126973 | 38.1 | 87.6 | x |
| AP-3472 | AP-2D | 122768 | 121483 | 42.7 | 88.8 | x |
| AP-3473 | AP-3D | 123597 | 135944 | 58.7 | 112.3 | x |
| AP-3475 | AP-5D | 120007 | 132433 | 51.8 | 102.4 | x |
| AP-3476 | AP-6D | 119955 | 134970 | 46.3 | 107.0 | x |
| AP-3477 | AP-7D | 121350 | 138425 | 53.0 | 116.8 | x |
| AP-3478 | AP-8D | 117665 | 137872 | 33.5 | 108.1 | x |
| AP-3479 | AP-9D | 114355 | 132889 | 24.2 | 94.7 | x |
| AP-3480 | AP-10D | 119117 | 124029 | 35.5 | 84.5 | x |
| AP-3482 | AP-12D | 112834 | 123149 | 32.0 | 75.2 | x |
| AP-3484 | AP-14D | 116022 | 129710 | 30.5 | 91.5 | x |
| AP-3485 | AP-15D | 114746 | 125290 | 32.0 | 81.1 | x |
| AP-3532 | AP-19D | 117990 | 128220 | 41.8 | 92.1 | x |
| AP-3534 | AP-21D | 117271 | 126617 | 41.1 | 87.2 | x |
| AP-3547 | B-62 | 122863 | 128326 | 47.9 | 96.4 | x |
| AP-3772 | | 116837 | 125871 | 35.7 | 84.9 | x |
| AP-3774 | | 117363 | 125605 | 34.4 | 85.9 | x |
| AP-3775 | | 117078 | 126233 | 34.1 | 85.8 | x |
| AP-3790 | | 117076 | 127494 | 24.5 | 89.1 | x |
| | | | **b. CRREL wells.** | | | |
| AP-3887 | BH-1 | 113198 | 128387 | 51.2 | 85.3 | x |
| AP-3888 | BH-2 | 120372 | 124686 | 52.5 | 87.1 | x |
| AP-3889 | BH-3 | 119247 | 132503 | 48.6 | 101.6 | x |
| AP-3890 | BH-4 | 121641 | 129785 | 51.7 | 97.8 | x |
| AP-3891 | BH-8 | 118646 | 125830 | 75.7 | 88.5 | x |
| AP-3892 | BH-9 | 115965 | 128569 | 52.2 | 89.7 | x |
| AP-3893 | BH-10a | 117298 | 128709 | 37.8 | 91.5 | |
| AP-3894 | BH-10 | 117298 | 128701 | 51.5 | 91.5 | x |
| AP-3895 | BH-11 | 117201 | 127502 | 51.5 | 89.2 | |
| AP-3896 | BH-11a | 117180 | 127528 | 38.4 | 89.2 | |
| AP-3897 | BH-12 | 116839 | 124433 | 56.7 | 82.5 | |
| AP-3898 | BH-12a | 116837 | 124443 | 36.9 | 82.5 | |
| AP-3899 | BH-14 | 115136 | 127306 | 38.1 | 86.2 | |
| AP-3900 | BH-15 | 114284 | 130142 | 55.0 | 89.3 | |
| AP-3901 | BH-16 | 116302 | 126907 | 38.5 | 87.0 | |
| AP-3902 | BH-16a | 116303 | 126912 | 52.9 | 87.0 | |
| AP-3903 | BH-18 | 118075 | 135346 | 56.2 | 103.3 | |
| AP-3904 | BH-19 | 119271 | 136835 | 52.9 | 108.4 | |
| AP-3905 | BH-20 | 121426 | 134754 | 71.1 | 108.9 | |
| AP-3906 | BH-23 | 116685 | 130406 | 53.2 | 93.8 | |
| AP-3908 | BH-9A | 115967 | 128582 | 52.2 | 89.7 | |
| AP-3909 | BH-25 | 115937 | 127441 | 51.4 | 87.1 | |
| AP-3910 | BH-25A | 115938 | 127431 | 39.3 | 87.1 | |
| AP-3911 | BH-27 | 117474 | 121258 | 51.8 | 76.6 | |
| AP-3912 | BH-28 | 119635 | 129672 | 52.1 | 96.1 | |
| AP-3913 | BH-29 | 125827 | 144507 | 27.8 | 142.4 | |
| AP-3914 | BH-30 | 117826 | 130749 | 39.9 | 96.0 | |
| AP-3915 | BH-31 | 106166 | 138107 | 21.5 | 135.1 | |
| AP-3916 | BH-24 | 117331 | 125831 | 47.4 | 85.4 | |

*x indicates that geophysical logging was done in this well.

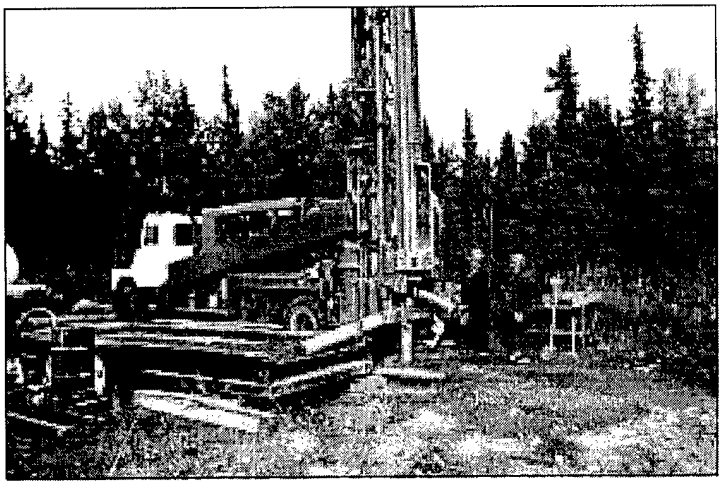

**Figure 6. Air rotary drill rig used by Ambler Exploration to drill boreholes for this study.**

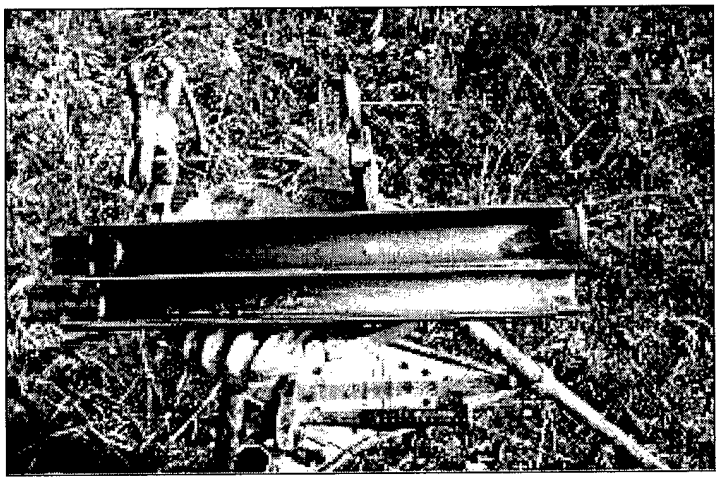

**Figure 7. Example of split-spoon sampler used to collect soil samples. (Quarter in center of sampler for scale.)**

sedimentary characteristics in the lithologic logs of 25 previously drilled boreholes.

## Downhole geophysics

Geophysical surveys within 32 boreholes were conducted in November 1997 by Terrasat, Inc., of Anchorage, Alaska. Natural gamma, electrical resistivity by electromagnetic induction, and fluid temperature were measured in 32 PVC-cased (approximately 5-cm i.d.) boreholes (Fig. 8). In addition, electrical resistivity, fluid temperature, fluid conductivity, and spontaneous potential were measured in a single uncased borehole (AP-3891) to a depth of 76 m in a thick gravel sequence north of Building 45-590 (Fig. 3b). It was open-hole logged to evaluate signal response in natural material, and later relogged to observe the effect of PVC casing on signal attenuation and response. We planned to examine a second uncased borehole in different materials, but it was not drilled because of equipment complications encountered during the drilling of AP-3891.

The sensors in the two geophysical tools we used respond to the physical properties of the soil and other material surrounding the borehole to provide precise, unbiased, and high-resolution data. Geophysical logs can then be interpreted using borehole logs and sample descriptions, which enable subsequent cross-correlation among boreholes. A brief description of each sensor and the nature of its response to geologic strata and natural properties is given below.

### *Electrical logs*

Electrical logs measure the natural potential and resistivity of the stratigraphic formations. They can only be run in uncased boreholes (Keys and MacCary 1971), with a conductive fluid being used to transmit an electric current to the formation. These logs provide quantitative information on formation resistivity and are

**Figure 8. Century Geophysical Corporation combination natural gamma and induction tool used in PVC cased boreholes.**

generally useful as stratigraphic indicators. Electrical logs collected in AP-3891 included short-normal and long-normal resistivity, spontaneous potential (SP), and lateral resistivity.

### *Short- and long-normal resistivity*

The apparent resistivity of the formation surrounding a monitoring well was measured using sensors that emit a high-frequency, alternating electrical current (Repsold 1989, Asquith and Gibson 1982). Two electrodes on short and long spacings record the electric potential, a property proportional to the formation resistivity. The shorter electrode spacing of 40.6 cm (short-normal) permits only shallow penetration of the electric current into the surrounding material, but provides good layer resolution (about 0.5 m thick). The longer electrode spacing of 162.6 cm (long-normal) produces deeper penetration and is useful for determining formation resistivity; however, its layer resolution is reduced (about 2 m). By combining these profiles, stratigraphic contacts and layer resistivity can be defined.

### *Spontaneous potential*

The spontaneous potential (SP) sensor measures the natural voltage potentials between borehole fluids and the surrounding formation in uncased boreholes (Keys and MacCary 1971). The SP tool records the direct current voltage difference between an electrode in the hole and one fixed at the surface (Asquith and Gibson 1982). The SP signal is primarily an electrochemical response to borehole fluids that have invaded the formation and geologic strata with meteoric water within them. The resulting logs are generally used for correlating geologic formations, determining layer thickness, and investigating the content of fine-grained particles.

### *Lateral resistivity*

This sensor is a three-electrode device consisting of two closely spaced voltage-measuring electrodes that are separated from a voltage source electrode. The device measures the difference between the two "equipotential spheres" defined by the radial distance between the source electrode and two measuring electrodes (i.e., a narrow zone between the two "spheres" at about 1.8 m is the effective area of measurement). The result is that the resistivity of a thin zone about 1.8 m away from the probe is measured with little interference from the borehole.

### *Induction*

The induction sensor measures electrical conductivity in the formation (in W-m) using a current generated by it (Asquith and Gibson 1982, Conlog 1990). The sensor induces an electromagnetic field in the formation and a secondary or induced field proportional to the formation's conductivity is generated. The induced field is recorded as a current in the receiver coil of the sensor. The signal response is coupled to the formation by the electromagnetic field and does not require transmission of a current through borehole fluids. Therefore, induction measurements may be made in either air- or fluid-filled holes, including holes cased with PVC. The transmitter/receiver spacing of the sensor is 101.6 cm, allowing beds of 1.5 m or thicker to be identified.

### *Natural gamma*

The natural gamma sensor uses a scintillation counter to measure gamma radiation emitted by the radioactive decay of minerals in the formation. The primary natural element emitting gamma radiation is the isotope potassium-40 present in clay minerals; however, isotopes of thorium and uranium can also be important sources. In sedimentary strata, radioactive minerals containing potassium tend to be concentrated in fine-grained, clay-rich horizons. These horizons exhibit higher radioactivity levels than coarser sediments without clay minerals. Gamma ray logs are, therefore, com-

monly used to identify lithologic units in water wells for correlating site stratigraphy. Since high energy gamma rays emitted from the formation penetrate both PVC and steel, this technique can be used in uncased or cased holes, either filled with liquid or air (Keys and MacCary 1971). This provides a distinct advantage over the electric logs that require a fluid-filled, uncased borehole for logging.

The gamma ray (GR) radiation recorded by the sensor is proportional to the weight concentrations of radioactive material in a formation according to

$$GR = \Sigma \rho_i V_i A_i / \rho_b$$

where

$\rho_i$ = density of the radioactive minerals
$V_i$ = bulk volume factor of the minerals
$A_i$ = proportionality factor corresponding to the mineral radioactivity
$\rho_b$ = formation bulk density (Schlumberger 1989).

Gamma rays are bursts of high-energy electromagnetic waves that are spontaneously emitted by radioactive elements. Along the gamma ray path, energy is dissipated into the formation and the gamma rays are gradually absorbed at a rate proportional to the formation density. Therefore, two formations with similar radioactivity, but different bulk density, will exhibit different radioactivity levels.

### *Fluid temperature*

High-resolution temperature changes in the borehole fluid are recorded using an electric resistance thermometer located at the bottom of the tool. If the water is undisturbed, the temperature profile provides a proxy for the temperature gradient in the surrounding materials. Temperature spikes as seen at AP-3532 may indicate a leak in the casing and local exchange of ground water.

## RESULTS

### Outcrops

Natural and artificial exposures reveal the characteristics of the near-surface sediments in the Mountain View fan. Typically, the gravels have varying amounts of silt and clay in their matrix, which appear in some places as isolated lenses or layers with higher moisture contents. Finer, well-sorted layers are common and appear to have been deposited in quiet water pools or abandoned channels while the Mountain View fan formed (cf. Jopling and McDonald 1975, Smith 1985). An example of a fine-grained horizon deposited in this way is the clay horizon in near-surface alluvial gravels at the Ruff Road Fire Training Pit (AP-3635 and AP-3639; Hunter et al. 1999).

Poorly sorted (well-graded) gravels are typical of Mountain View fan deposits. An outcrop of about 8 m of stratified sand and gravel occurs in a gravel pit between Bryant Air Field and Camp Carroll (Fig. 3b). The upper level on the north side of the pit reveals 3 m of stratified gravel (Fig. 9). Here, the individual layers range from generally massive (unstructured) to cross-bedded, with graded to sharp erosional contacts (Fig. 10 and 11). The upper 0.5 m and lower 1 m consist of poorly sorted, matrix-supported gravel with a silty/

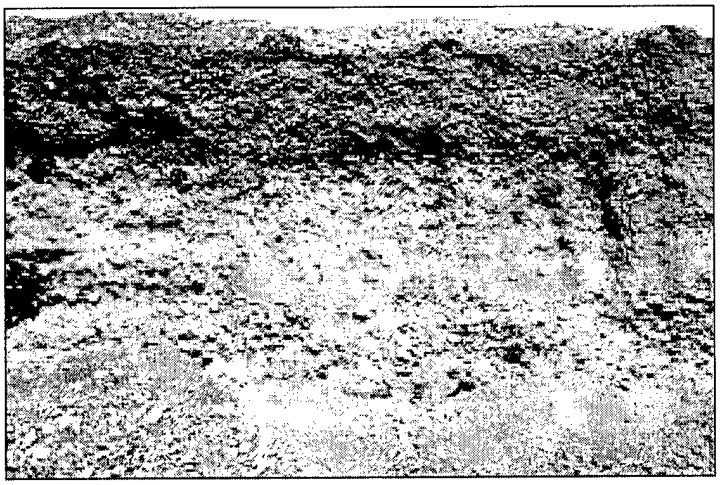

**Figure 9. Stratified gravel exposure in the upper section of the Bryant Air Field gravel pit.**

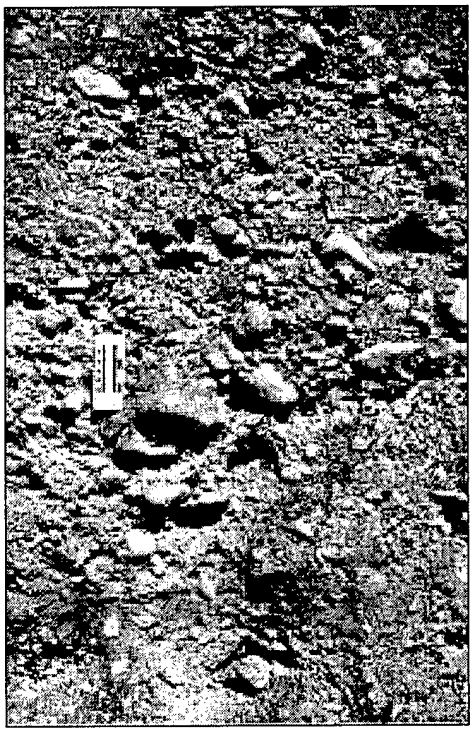

**Figure 10. Close-up of coarse, generally structureless, gravel at base of sequence shown in Figure 9.**

sandy matrix (Fig. 12). The middle 1.5 m consists of a series of small cut-and-fill sequences with normally graded, clast-supported gravels and open-framework (no matrix) gravel lenses (Fig. 13). The lower levels of the outcrop show plane-bedded gravels, with interbeds of sand and silty sand (Fig. 14 and 15). Silt content generally increases with depth, while localized silt-rich horizons impede downward percolation of water and create seeps in the pit wall (Fig. 16). These are characteristic of proglacial stream deposits, where rapid vertical and lateral changes in grain size and structure are common (e.g., Rust 1975, Smith 1985).

A sandy gravel occurs at the top of the Mountain View fan sequence. It is exposed in a foxhole on the training grounds just east of Fourth Street, between AP-3892 and AP-3893 (Fig. 3 and 17). A 1-m-thick layer of loess-rich, silty sand lies on top of the sandy gravel (Fig. 18). The silty sand grades downward into sand with scattered gravel and eventually to a coarse gravel at 0.3 m depth. Alternating matrix- and clast-supported coarse gravels extend to 0.6 and 0.7 m depth, where there is a cobble layer. The lowermost 0.3 m of the section consists of a clast-supported pebbly gravel, with thin horizons of pebbles without a fine-grained matrix (i.e., open framework).

A riverbank on Ship Creek, south of the Water Treatment Plant (Building 28-008; Fig. 3b), exposes a 22-m section of the near-surface materials (Fig. 19 and 20) that are typical of the sediments of the Mountain View fan. The sedimentary sequence consists of a 1.5-m cap of wind-blown silt (i.e., loess) that unconformably overlies stratified gravel, interbedded with sand horizons (Fig. 21 to 23). Below the gravel, a poorly sorted diamicton with a silty–sandy matrix forms a southerly pinching lens (Fig. 24). The lens appears to be the nose (or snout) of a former debris flow, which moved over the silt, sand, and gravel deposits (Fig. 20 and 21). The sand is deformed beneath the diamicton, showing that it was probably saturated when buried by the flow (Fig.

**Figure 11. Poorly sorted gravel with cross beds, normal grading, and erosional contacts.**

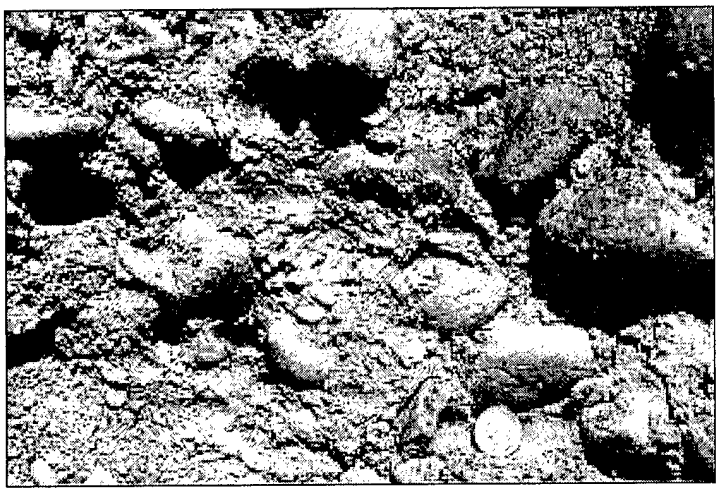

Figure 12. Poorly sorted, matrix-supported gravel with a silty/sandy matrix.

Figure 13. Normally graded, open-framework gravel (center of photo above pen).

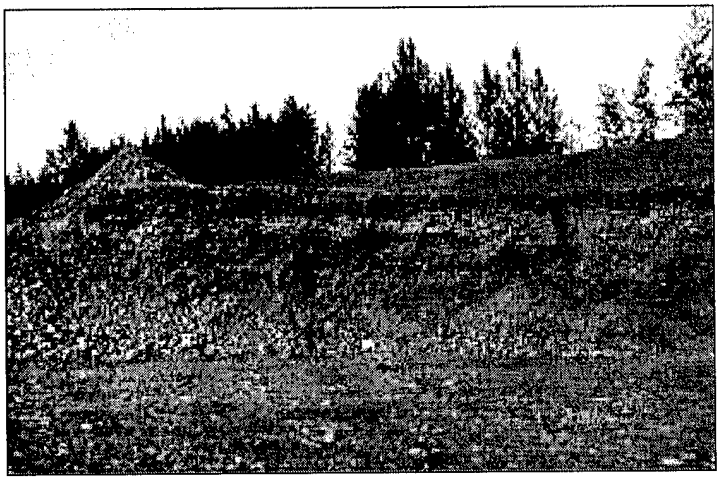

Figure 14. Northeast wall in lower section of the Bryant Air Field gravel pit. Stratification is generally planar with interbeds of sand.

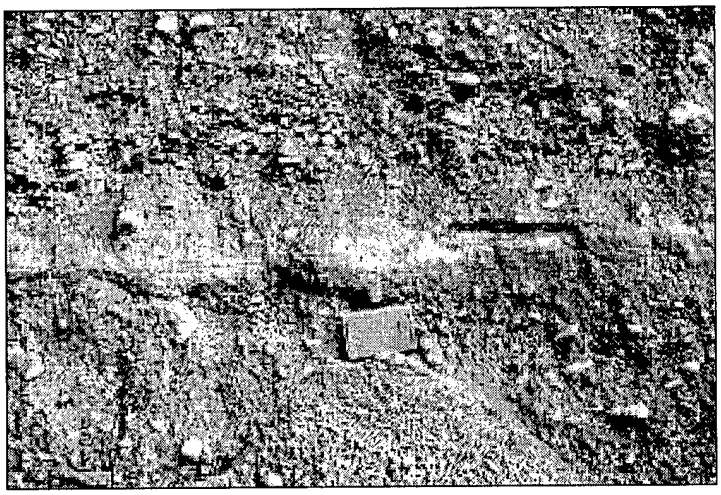

**Figure 15. Planar bedded sand interbedded within clast-supported gravel.**

25). The sand is located above a horizontally bedded silty sand that coarsens with depth (normally graded) and exhibits cross-bedding. A 1- to 1.5-m layer of truncated silt lies beneath the silty sand (Fig. 21). The lower 6 m of the sequence consists of coarse, clast-supported gravel with a weak stratification (Fig. 19, 21 and 26).

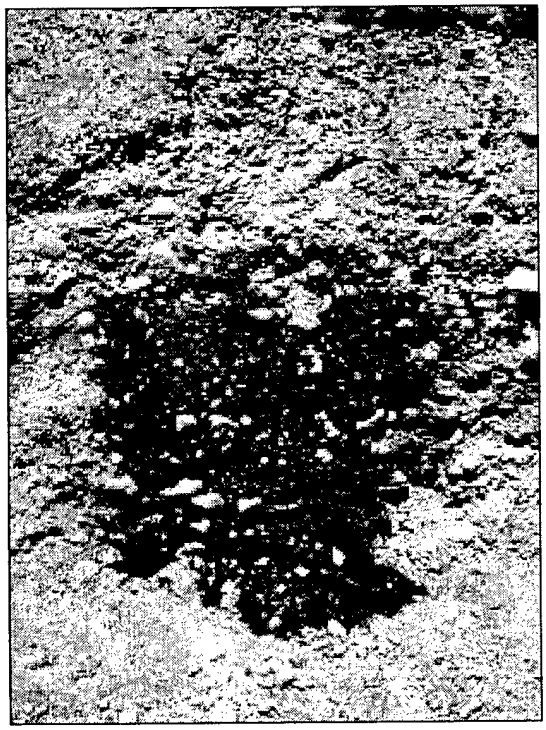

**Figure 16. Ground water seep from top of silt-rich layer within poorly sorted gravel.**

Borehole logs

The boreholes drilled in 1997 and 1998 ranged from 21 to 76 m in depth, but only one (AP-3905) encountered bedrock. At that site, the bedrock consists of a saprolite with extensive weathering and alteration of minerals to clays. The basic sediment types encountered are fine silt and clay, sand, gravel, and diamicton.

*Silt and clay*

Distinct horizons of silt and clay are minor but stratigraphically important components of the subsurface materials. They typically make up less than 10% of a section, but occasionally as much as 30% (AP-3903). Although a minor constituent, clay and silt beds have lower permeability than the coarser sand and gravels, and, therefore, can impede the vertical movement of ground water. Generally, silt and clay horizons are thinly laminated. The laminae consists of normally graded clay, silt, and sand couplets of 1- to 10-mm thickness (Fig. 27 and 28). In boreholes AP-3892, AP-3894, and AP-3902, a thinly laminated clay coarsens upward (inverse grading) to a sandy silt. Where clay is present at the bottom of a sequence, it is typically dense and brittle, with a high plasticity. Silt horizons may be weakly cross-bedded or deformed.

*Sand*

Sand horizons are commonly encountered in the subsurface, where they compose up to 38% of a sequence. The thickness of sand horizons ranges from a few tens of centimeters to tens of meters. Typically, sands are moderately to poorly sorted, with medium to coarse sand being slightly more abundant than gravel clasts (Fig. 29). Sand units that are less than 1 m thick are often interbedded with sandy gravels. These

**Figure 17. Foxhole containing exposure of upper gravel in Mountain View fan.**

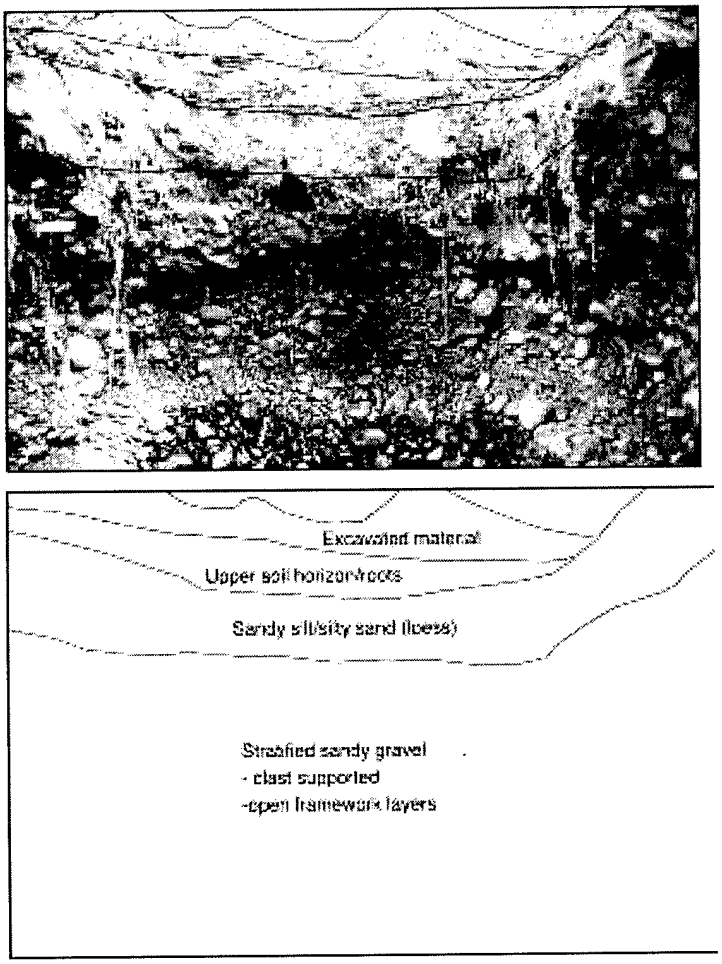


**Figure 18. Foxhole exposure and interpretation: coarse, clast-supported gravel overlain by thin, windblown silt (loess).**

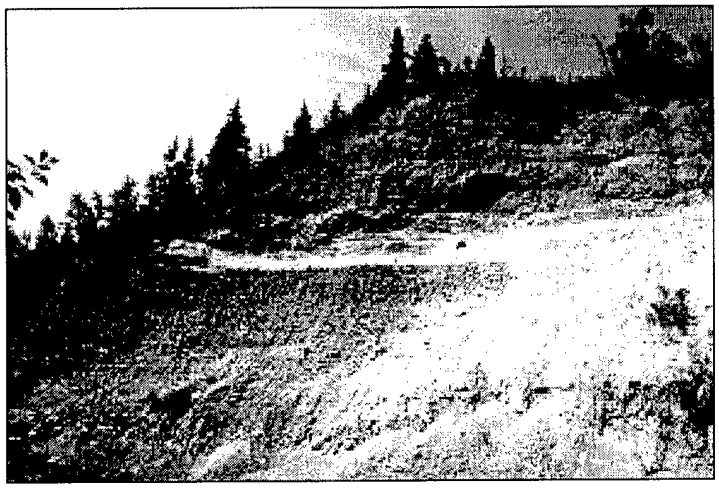

**Figure 19. River cut along Ship Creek near Fort Richardson Water Treatment Plant.**

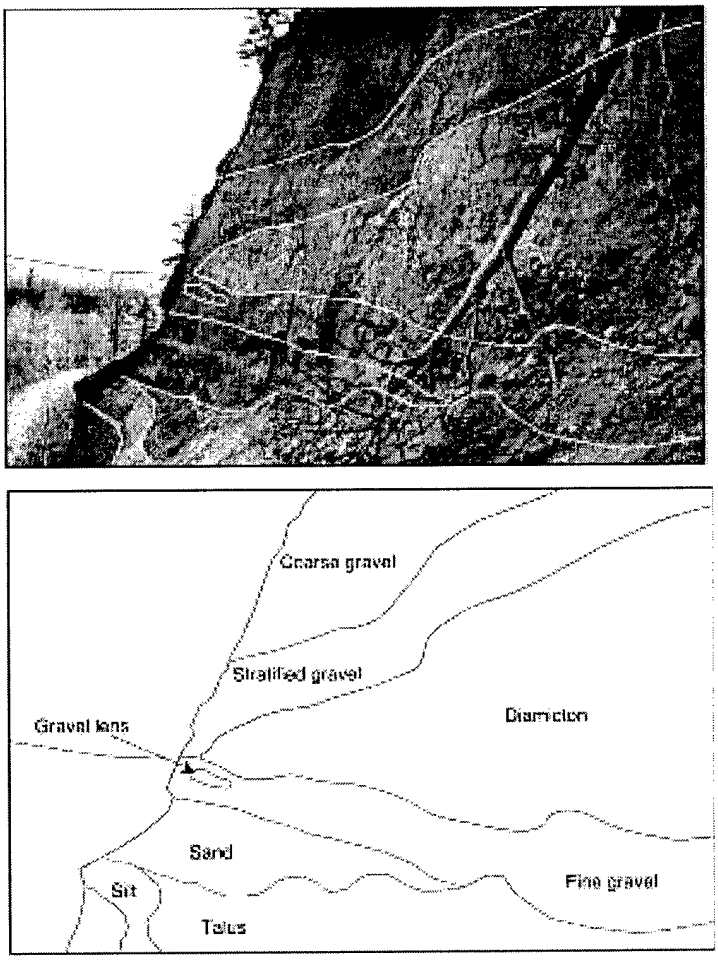


**Figure 20. Oblique view of the upper section of the river cut showing the nose of apparent debris flow.**

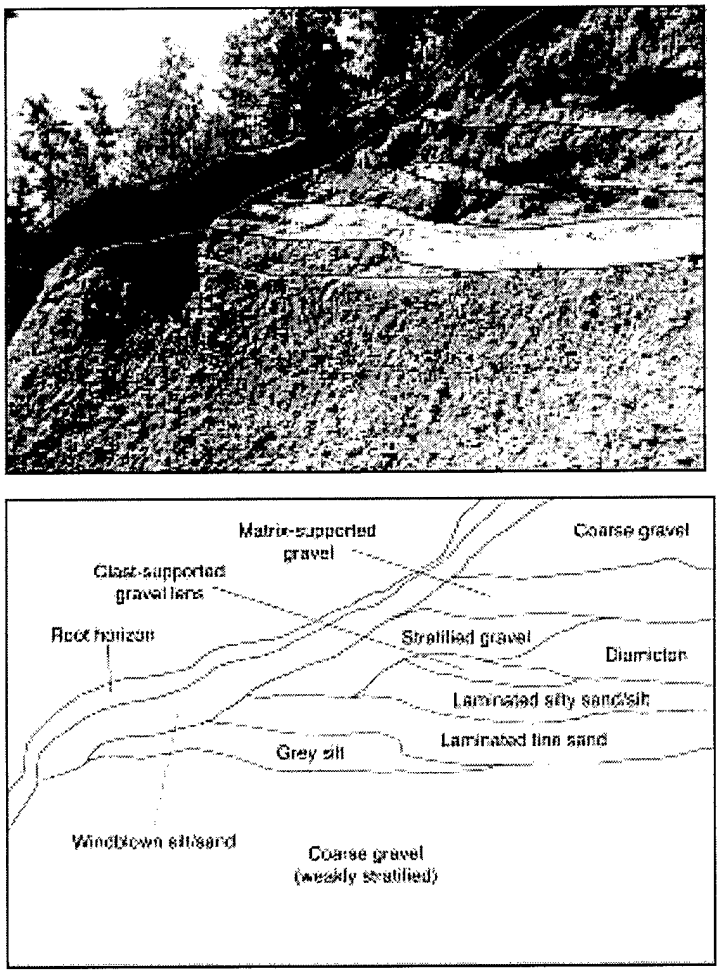


**Figure 21. View of Ship Creek section shown in Figure 19, having deformed sand below debris flow deposits. The entire section is capped by a 1.5-m-thick loess deposit.**

interbedded sand–gravel units are common in the Mountain View fan.

Well-sorted sands are not as common, but form distinct horizons where they are found. The well-sorted medium sand, such as in AP-3889, ranges from generally unstructured (Fig. 30) to thinly bedded (Fig. 31). Near its upper contact, the medium sand is thinly interlaminated with silt and fine sand (Fig. 31). The lower part of the horizon behaves thixitropically and heaves during drilling. Thin-bedded sand, or sand with silt and clay laminae, occurs at the top of a coarsening upward silt and clay sequence in AP-3892, AP-3894, AP-3902, and AP-3903. Thin stringers of clast-supported granular gravels are also common in sandy horizons (e.g., AP-3903 and AP-3906).

*Gravel*

Gravel is common and makes up 39% to more than 90% of the sedimentary sequences of boreholes in the cantonment area. Gravels are usually poorly sorted, with particles ranging in size from pebbles to coarse cobbles and boulders (Fig. 32 and 33). Clasts tend to be spherical and rounded to well-rounded, indicating their fluvial origin. The gravel's matrix is highly variable in size, ranging from clay- or silt-rich sand to well-sorted, angular granules. Most of the gravels are clast-supported and occasionally exhibit an open framework. Stratification was difficult to observe in the disturbed split-spoon samples from boreholes; however, thin beds of sand or silt could be seen. Textural changes (coarse vs. fine) in consecutive samples suggest that a weak strati-

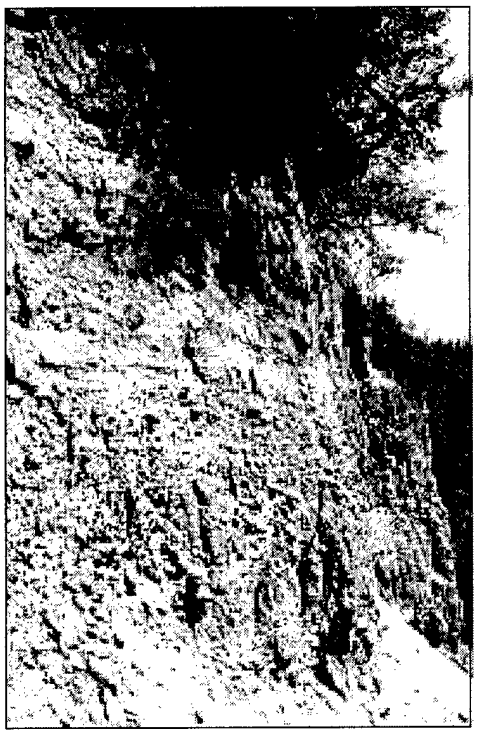

Figure 22. Uppermost gravel, looking north at top of section. Gravels are stratified with interbeds of silty-sand and sand.

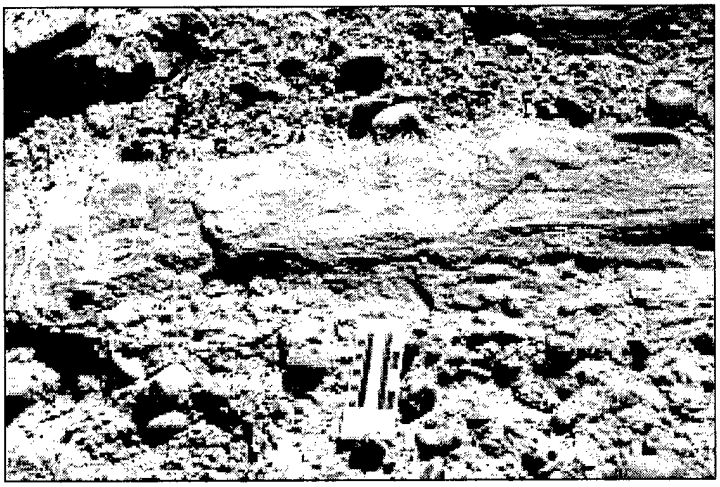

Figure 23. Close-up of planar bedded and cross bedded sand strata within gravel sequence shown in Figure 22.

Figure 24. Poorly sorted, matrix-supported diamicton within apparent debris flow shown in Figure 20.

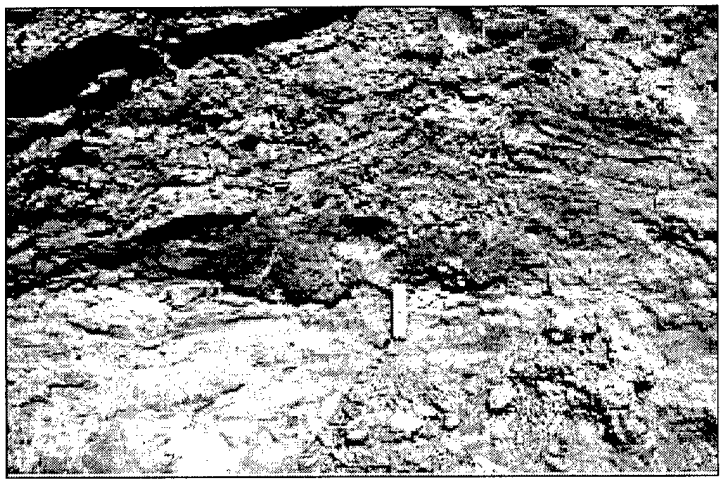

Figure 25. Deformed and disaggregated (breccia) silt and sand found at base of diamicton.

Figure 26. Poorly sorted sandy gravel found at base of Ship Creek section. Gravel is generally unstructured; however, cobble- and boulder-rich horizons show a weak stratification.

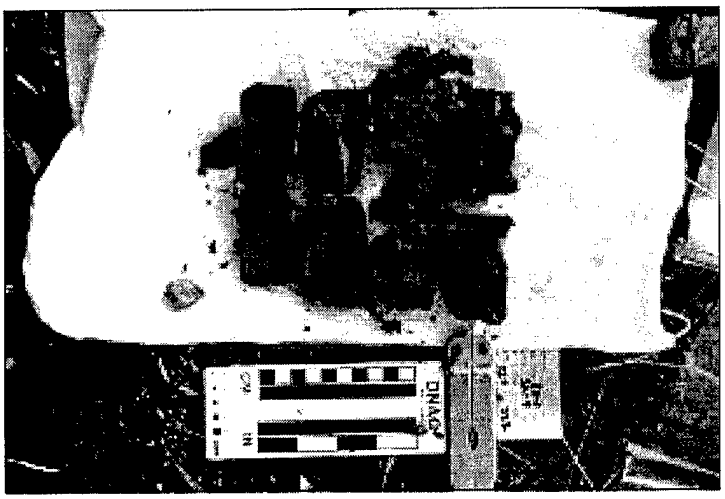

Figure 27. Thinly laminated silt found in sample 7 at AP-3887.

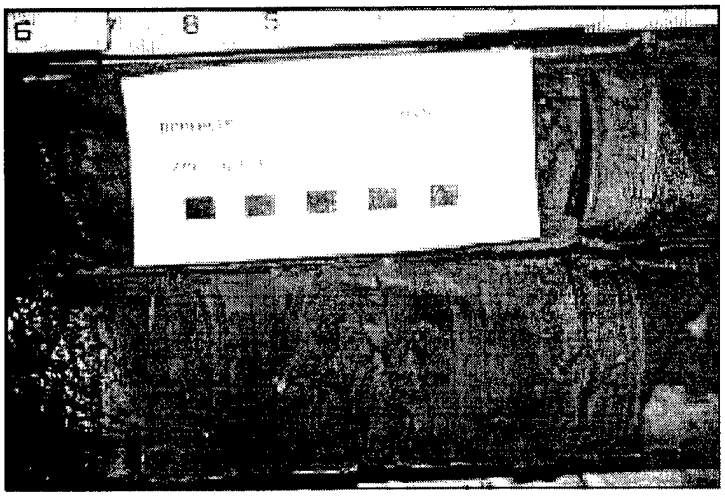

Figure 28. Thinly laminated silt found in sample 14 at AP-3903.

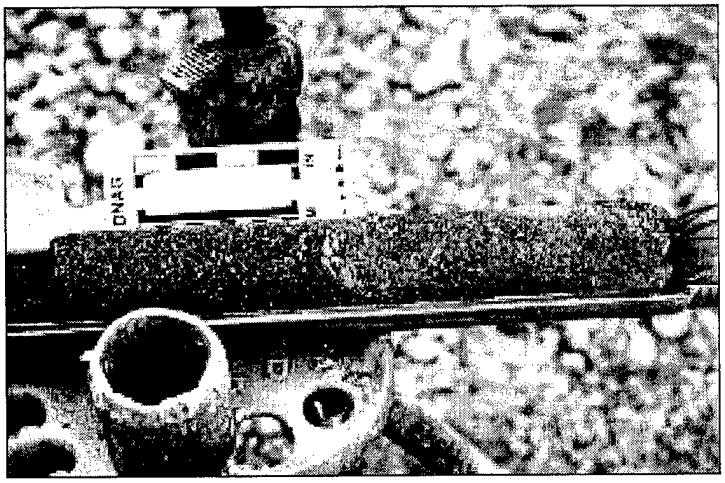

Figure 29. Split-spoon sample collected at AP-3888 in sample 14 showing coarse gravelly sand (left half of sample) and closely associated sandy gravel.

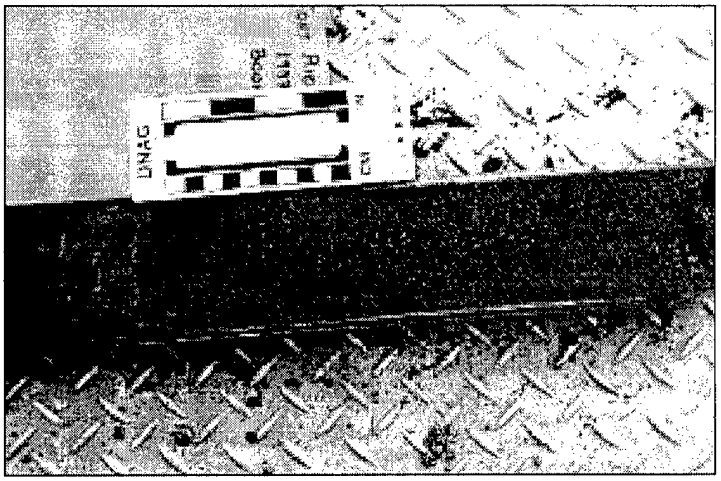

Figure 30. Well-sorted medium sand and thinly laminated silty sand (6 cm at left of photo) collected in sample 11 (AP-3889).

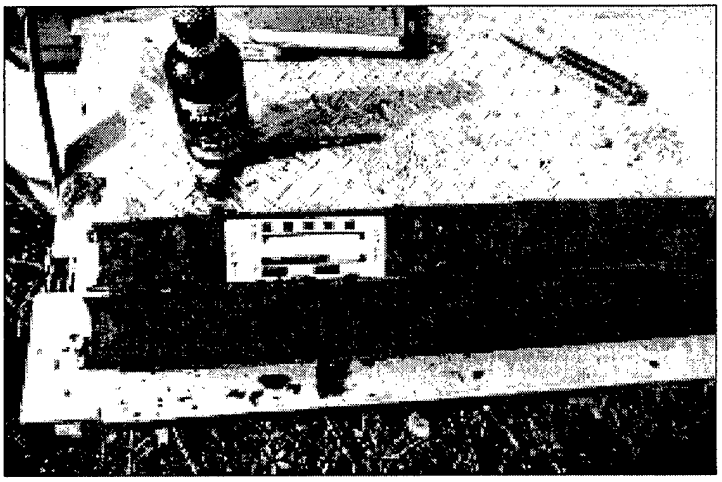

Figure 31. Well-sorted medium sand with well-preserved bedding (Sample 13, AP-3889).

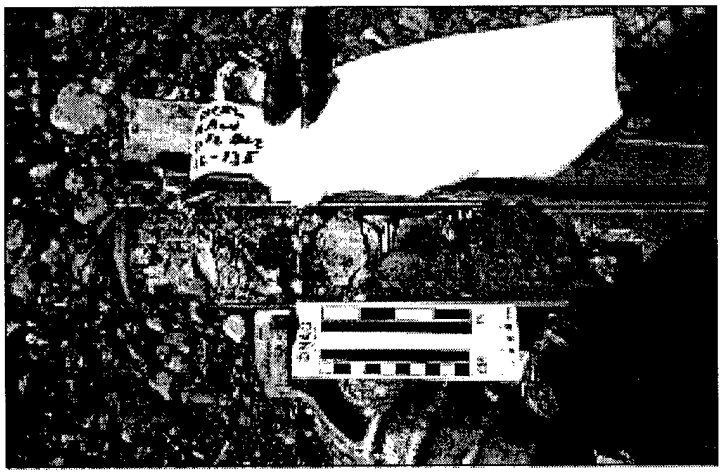

Figure 32. Poorly sorted gravel retrieved in sample 2 of AP-3888. Coarse, angular fragments in center of core are pieces of fractured cobble broken when sampler was driven into soil.

**Figure 33. Samples 11 through 13 (left to right) from AP-3887 showing textural variability in the poorly sorted gravels. Variability reflects weak stratification in subsurface.**

fication exists (Fig. 33), representing fluctuating stream discharge and migrating channels at the time of deposition.

Where well-defined stratification exists, its presence is defined by smaller clast sizes (i.e., pebbles vs. cobbles) or finer matrices (i.e., clayey silt vs. granular sand). At some locations, varying percentages of sand and gravel also produce alternating layers of sandy gravel and gravelly sand (e.g., AP-3891). Grain-size analyses suggest that a typical composition might range from 1 to 13% fines, 13 to 44% sand, and 47 to 74% gravel.

### *Diamicton*

Diamictons are texturally diverse and form a second potentially important type of material that can confine ground water movement below the canton-ment. These diamictons are commonly moderately to poorly sorted and matrix supported (Fig. 34 to 36). Stratified, clast-supported diamictons are relatively rare, but were observed as a transitional phase at some contacts between gravel and diamicton (e.g., AP-3892 at 32 m). These particular gravels have sand-rich matrices and very high gravel contents.

Most often, diamicton observed during drilling contained 12 to 60% gravel, 26 to 45% sand, and 15 to 50% fines. Stratified diamictons observed in AP-3889, AP-3900, AP-3892, and AP-3902 generally have higher gravel contents (~50 to 60%) and less silt (5 to 16%).

Matrix-supported diamictons contain various amounts of sand, silt, and clay. Gravel clasts are typically subangular to subrounded, with little or no preferred orientation. Often, such diamictons are not overconsolidated and clasts have abraded faces. Most of these diamictons are probably deposits of debris flows that are commonly active along glacier margins (Lawson 1979, 1988, 1993).

Denser diamictons (i.e., highly compacted) contain abraded and "bullet-shaped" clasts with striated facets. These diamictons are usually unstructured or massive, but may contain silt stringers and exhibit a strong fissility (Fig. 35 and 36). Their matrices range from highly plastic, clay-rich silt to silty sand. Such diamictons are believed to be produced by subglacial lodgement, or, when more limited in extent and thickness, may be deposits of debris flows that originated in other glacial deposits.

A unique class of diamicton exists that contains little gravel (2 to 22%) and is abundant in fines (clay and silt of 60 to 95%). It is classified as a pebbly mud (i.e., Jackson 1997). Clasts in these diamictons, which typically range from granule to pebble size, are floating in the clayey silt or silty sand matrix (Fig. 37 and 38). Often, these pebbly muds have thin (0.1- to 2.5-cm) laminations of clay, silt, or sand (e.g. AP-3887 from 9–11 m; AP-3894 from 28–35 m; Fig. 37 to 41). Pebbly muds originate in the marine environment near glaciers where clasts are deposited by their release from icebergs generated at the tidewater glacier margin (e.g., Thomas and Connell 1985, Dowdeswell and Dowdeswell 1989, Gilbert 1990, Hunter et al. 1996a). The concentration of clasts varies to such a degree that lateral correlation of units is difficult.

a. Sample 19 in AP-3890.


b. Sample 29 in AP-3887.

Figure 34. Poorly sorted, matrix-supported sandy-silty diamicton.

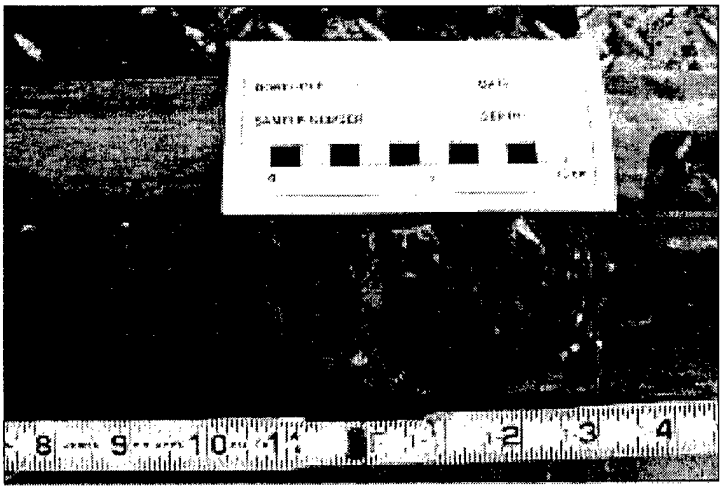

Figure 35. Close-up of poorly sorted diamicton (sample 11, AP-3895). Sample has fractured because of a well-developed fissility in the sample.

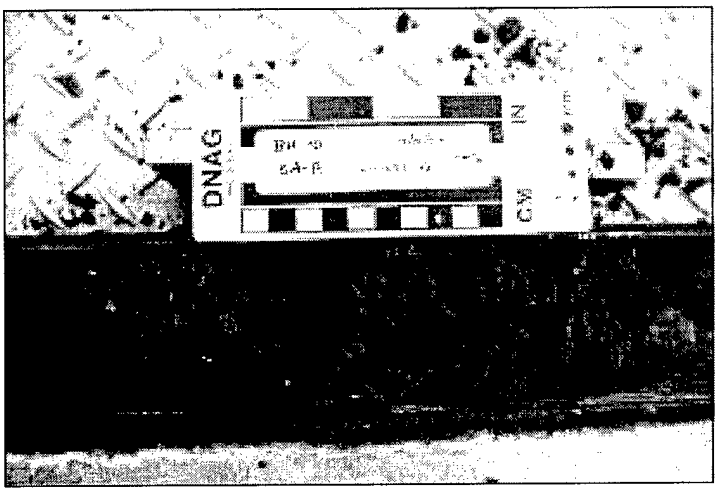


a. Close-up of split sample showing a well-developed fissility.

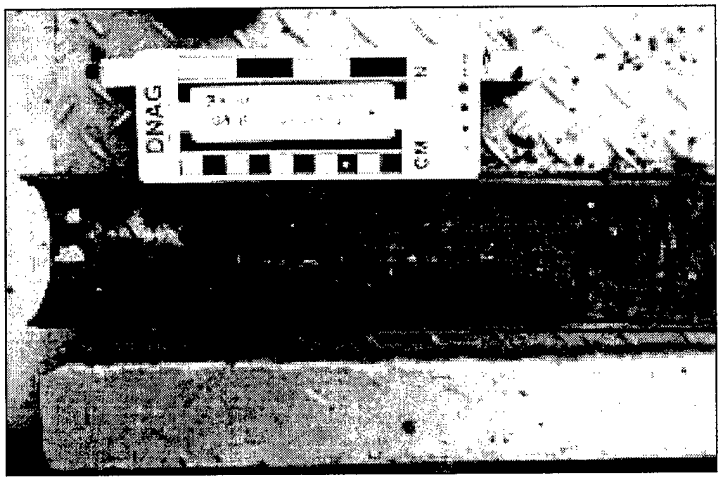


b. Close-up of undisturbed sample. Material is compact and tight.

Figure 36. Poorly sorted, matrix-supported silty diamicton.

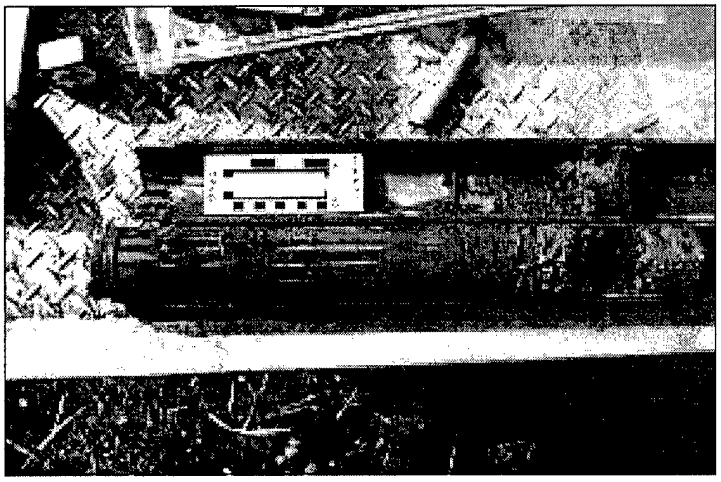

a. Freshly opened split-spoon showing dense mud.

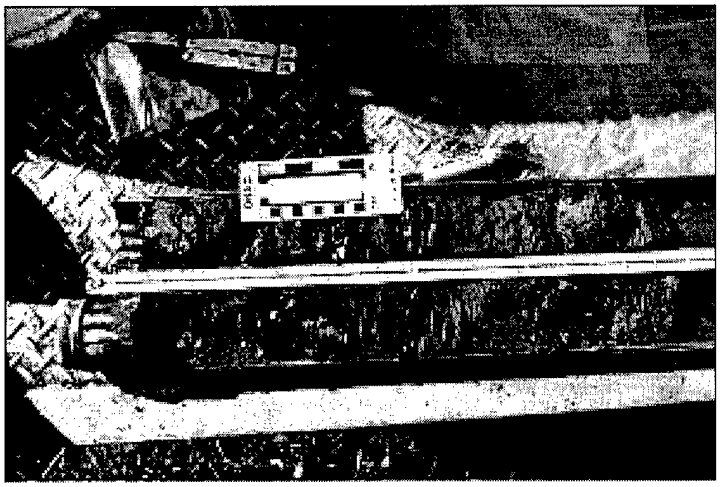

b. Split sample showing a brittle, laminated silt.

Figure 37. Pebbly mud retrieved in sample 15 from AP-3889.


Figure 38. Close-up of AP-3889 sample 15 showing granules and pebbles and outsized clasts embedded within laminated silt.

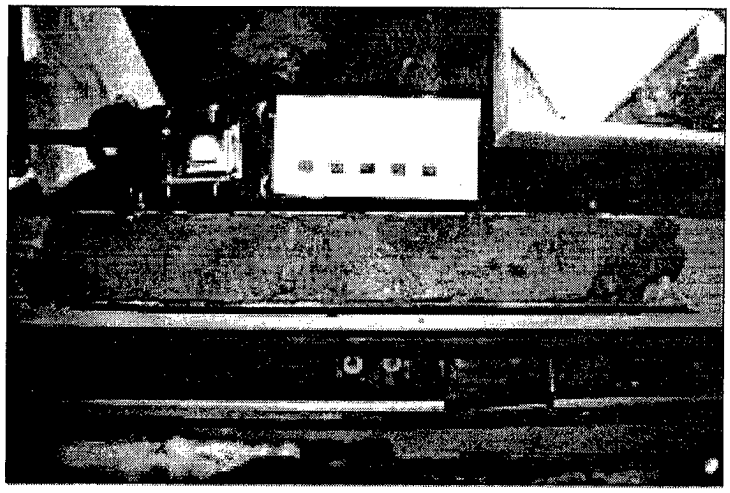

Figure 39. Sample 21 of AP-3895 showing moist pebbly mud.

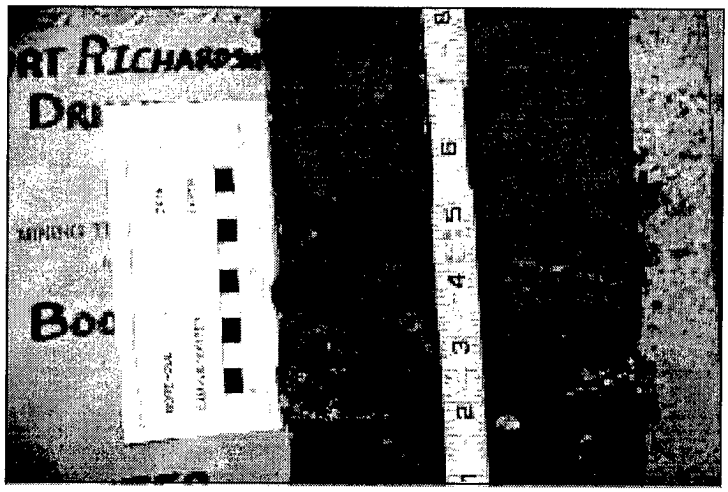

Figure 40. Silty pebbly mud retrieved in sample 6, AP-3909. Silts are thinly laminated with some sand laminae.

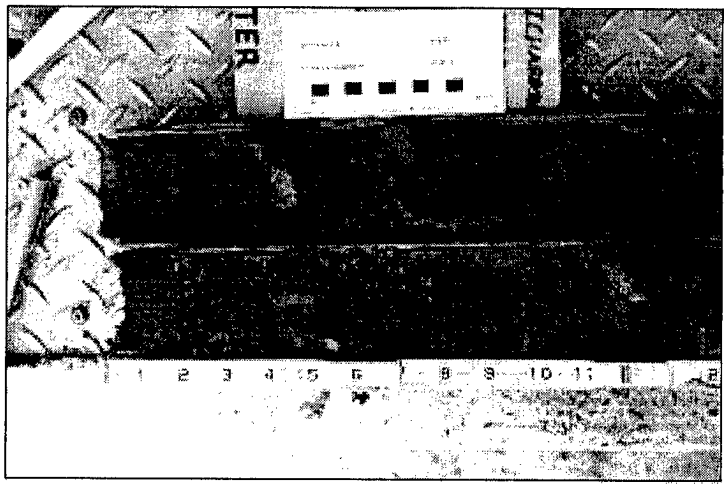

Figure 41. Dry, brittle pebbly mud retrieved in sample 16, AP-3909.

## Geophysical logs

The signal responses recorded by the downhole geophysical tools reflect the physical characteristics of sediment adjacent to each borehole. Patterns in the signal response in a series of well logs can be used to identify distinct depositional layers below the surface, and for correlation among the boreholes. These data are critical to resolving three-dimensional relationships among sedimentary layers and, thereby, defining the shape and extent of aquifers that control ground water flow patterns.

We evaluate signal response from the geophysical tools by comparing soil, lithologic, and completion logs and analyzing signal patterns recorded by tool sensors (Hunter et al. 1999). The typical responses for the induction tool, used on all of the cased boreholes and monitoring wells, include high gamma counts and moderate to high electrical conductivities for layers with an abundance of clay (e.g., clay, pebbly mud, clay-rich diamicton, and gravel with a clay-rich matrix) (Table 3); low gamma counts and low to moderate conductivities for well-sorted silt; and low to moderate gamma counts and generally moderate conductivities for sand and gravel. The combined response of natural gamma and electrical logging tools used on the uncased borehole (AP-3891) is described later.

### *Geophysical log complications*

Absolute values for natural gamma radiation are not used to quantitatively characterize the individual strata in monitoring wells because the natural gamma count is amplified by radioactive potassium in the bentonite grout (e.g., AP-3220, AP-3461, AP-3462, AP-3463, and AP-3547), the volclay grout above the screen, and the bentonite plugs (Fig. 42). However, patterns in gamma counts are useful for defining changes in the stratigraphy and correlating horizons among wells. Signal response is complicated in a different way in the zone where the screen and sand pack are present. Here, the gamma counts are relatively low because of the clean sand placed around the screen. The stainless steel screen can also locally intensify the conductivity values. Wells with PVC screens do not have this response (AP-3461, AP-3462, AP 3463, AP-3772, AP-3774, AP-3775, and AP-3790).

### *Cased-borehole interpretations*

In the 31 cased-boreholes and monitoring wells logged with the induction tool (e.g., Fig. 42), there is often a pronounced high gamma count representing the upper 3 m of sediment (e.g., AP-3375, AP-3462, AP-3477, AP-3484, AP-3772, AP-3774, AP-3887, AP-3889, AP-3890, AP-3891, AP-3892, and AP-3894). This zone is also associated with high conductivity levels that may

**Table 3. Relative geophysical response in cased boreholes.**

| *Sediment type* | *Natural gamma (in CPS)* | *Conductivity (mmho/m)* |
|---|---|---|
| Clay | High | Moderate |
| Silt | Low | Low to moderate |
| Sand | | |
| Silty sand | Low | Moderate |
| Clayey sand | Moderate | Moderate to high |
| Sand | Low | Low to moderate |
| Sand with gravel | Low to moderate with broad cycling | Low to moderate with broad cycling |
| Gravel | | |
| Sandy gravel | Low to moderate with broad cycling | Low to moderate with broad cycling |
| Silty gravel (near surface) | Moderate to high; broad cycling | Moderate to high with sharp peaks |
| Interbedded sandy gravel and gravelly sand | Moderate; well-developed cyclic reflecting alternating beds | Low to moderate; well-developed cyclic reflecting alternating beds |
| Gravel with silty/sand matrix | Low to moderate; weak cycling | Low to moderate; moderate cycling |
| Gravel with clayey matrix | High; moderate cycling | High; well developed peaks |
| Diamicton | | |
| Pebbly mud | High | Moderate to high |
| Clay-rich | High | Moderate to high |
| Silty diamicton | Low to moderate | Moderate; broad cycling |
| Sandy diamicton | Moderate | Moderate to high |

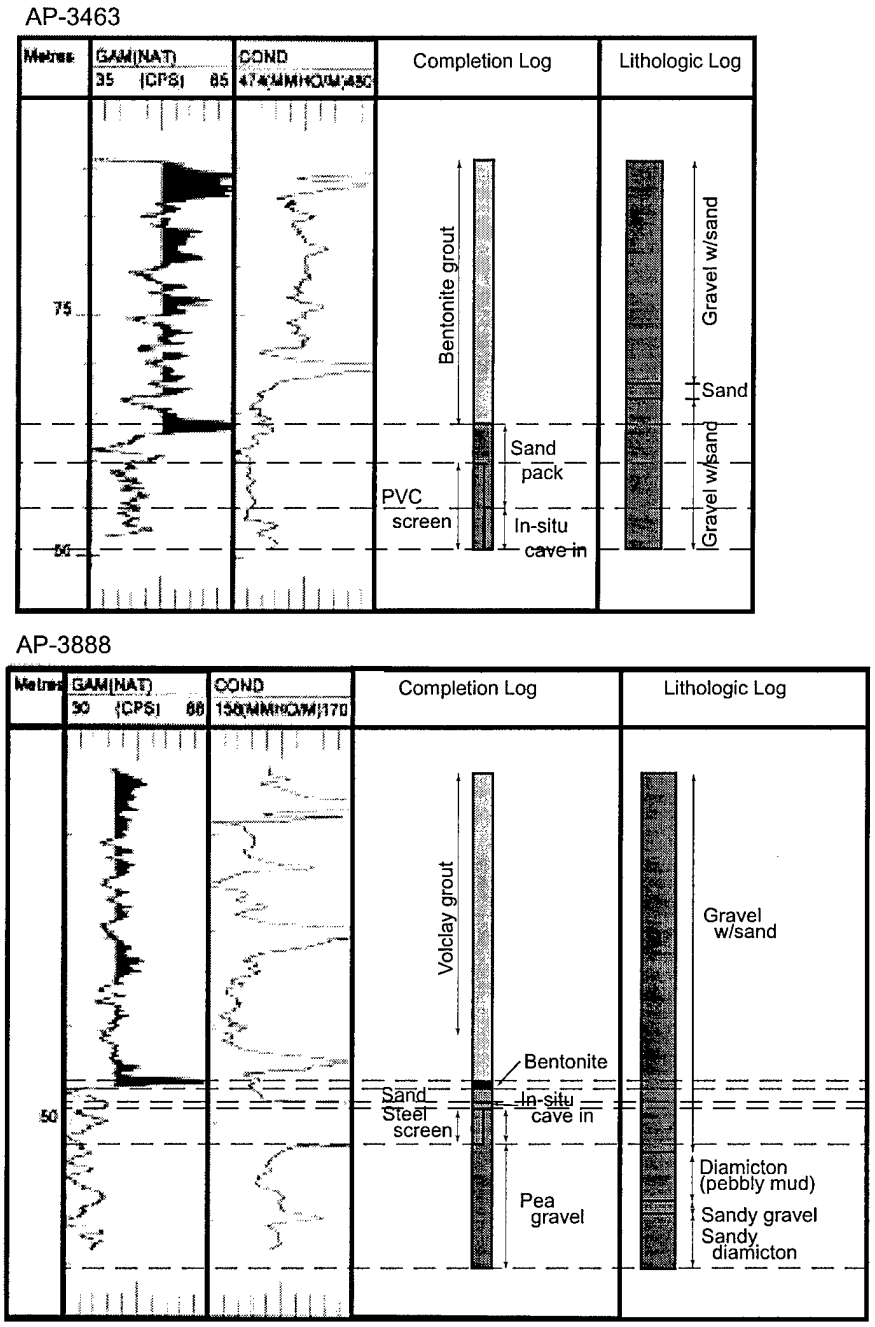


**Figure 42. Comparison of geophysical, well completion, and lithologic logs for AP-3469 and A-3888. Natural gamma counts decrease in both wells below the base of the grout. A sharp increase in conductivity in AP-3888 reflects the stainless steel screen placed near the bottom of the well.**

be in part a response to the windblown silt overlying the gravel, as noted in surface and river bank exposures (Fig. 22 and 23). However, the uppermost high values in conductivity and gamma count are often the highest in this 3-m-thick zone and likely reflect the tool passing the metal monument of the monitoring well and a bentonite plug at the surface.

Below 3 m, gravels with generally high gamma and moderately high conductivity values are encountered. Gravels occur in a zone ranging from roughly 3 to 10 m depth and are characterized by pronounced, high-amplitude cycling or broad cycles with superimposed noise that reflect the stochastic nature of gamma particle emissions; however, nearly 30 m of gravel with alternating high gamma counts exists at AP-3461. These upper gravels are typically cleaner than lower gravel units (Schmoll et al. 1996) and have a higher conductivity and gamma count. A noted exception is AP-3482, where the high gamma zone in the upper 10 m is absent. Its absence may be attributable to erosion by the meandering of Ship Creek.

There is a distinct zone of low gamma counts and moderate to high conductivity values in AP-3472, AP-3477, AP-3532, AP-3547, and AP-3889, below the upper gravel layer. This zone appears to represent a coarse, cobble-rich, sandy gravel horizon within the Mountain View fan deposits. Although not as distinct, gravels with low gamma counts in AP-3473, AP-3534, AP-3533, AP-3772, AP-3775, and AP-3894 may correlate with it. However, often the units underlying these latter gravels have moderate gamma counts with a regular cycling pattern, which indicates alternating sedimentary layers. For this reason, we interpret the zone as a unit of alternating sandy gravel and gravelly sand (e.g., AP-3775). The interbedded sandy gravel and gravelly sand is extensive throughout the study area, also being observed in AP-3462, AP-3463, AP-3475, AP-3476, AP-3479, AP-3480 AP-3485, and AP-3790. It reaches a thickness of 30 to 33 m in AP-3473, AP-3475, AP-3476, AP-3477, and AP-3890. Other gravels with low to moderate gamma counts and generally moderate conductivity values are common at greater depths in many boreholes.

Sand, silty sand, and gravelly sand typically had low gamma counts (AP-3462, AP-3476, and AP-3482). The conductivity values associated with these units are also typically low. However, an exception exists where high spikes in both conductivity and temperature occur in a sandy layer at about 73 m elevation (approximately 17 m depth) in AP-3892. This response likely reflects the presence of ground water with a high ionic content, which makes the water relatively conductive.

The geophysical response of diamictons is complex, reflecting their variable texture and composition. Silty and sandy diamicton horizons (tills and debris flows) in AP-3478, AP-3533, AP-3892, and AP-3894 have low to medium gamma counts and variable conductivity values. The more clay-rich, pebbly muds typically have higher gamma values than the coarser diamictons (e.g., AP-3478, AP-3887, and AP-3894) and the same general signature as laminated clayey silt and silty clay (e.g. AP-3889).

In many of the wells (AP-3220, AP-3469, AP-3475, AP-3476, AP-3478, AP-3479, AP-3482, AP-3484, AP-3485, AP-3772, AP-3888, AP-3889, AP-3890, and AP-3894), diamicton or pebbly mud was encountered at or near the bottom of the borehole. In these instances, their geophysical characteristics are generally masked by the alteration in signal response caused by the sand pack and well screen. Although stratigraphic contacts can still be determined from changes in the geophysical response, sample descriptions are the primary source of information on units in the bottom 3 to 10 m of a monitoring well (AP-3475, AP-3476, AP-3478, AP-3484, AP-3772, AP-3890, and AP-3894).

### *Open-hole log of AP-3891*

The open-hole logging of AP-3891 delineates 66 m of gravel, 5 m of sand between 49 and 54 m depth, and 5 m of diamicton at the base of the borehole (71 m depth) (Fig. 43). The low gamma counts and high conductivity values from the surface down to 15 m are a response to drill casing left to keep the borehole open prior to the logging exercise. The gamma, spontaneous potential (SP), resistivity, and conductivity values between 30 and 37 m depth represent a zone where the well diameter increased from 0.15 m to nearly 0.50 m. This was caused by loose sandy gravel being washed out during the drilling process. The start of the log traces for fluid resistivity, SP, short- and long normal resistivity, and lateral resistivity at 30 m depth tells us the location of the water table at the time of logging. A sand horizon from about 48 to 53 m depth has moderately lower gamma counts, higher SP, and lower resistivity in the short-normal relative to long-normal values, as well as a higher conductivity. Clays were not encountered in this borehole. The diamicton at the base of the borehole was not adequately sampled by the geophysical tools to allow us to geophysically characterize it.

## STRATIGRAPHIC UNITS

To simplify our interpretation, we have subdivided the sediments observed into 14 stratigraphic units on the basis of sample descriptions, geophysical logs, and vertical position (Fig. 44 to 49). The lowermost unit is

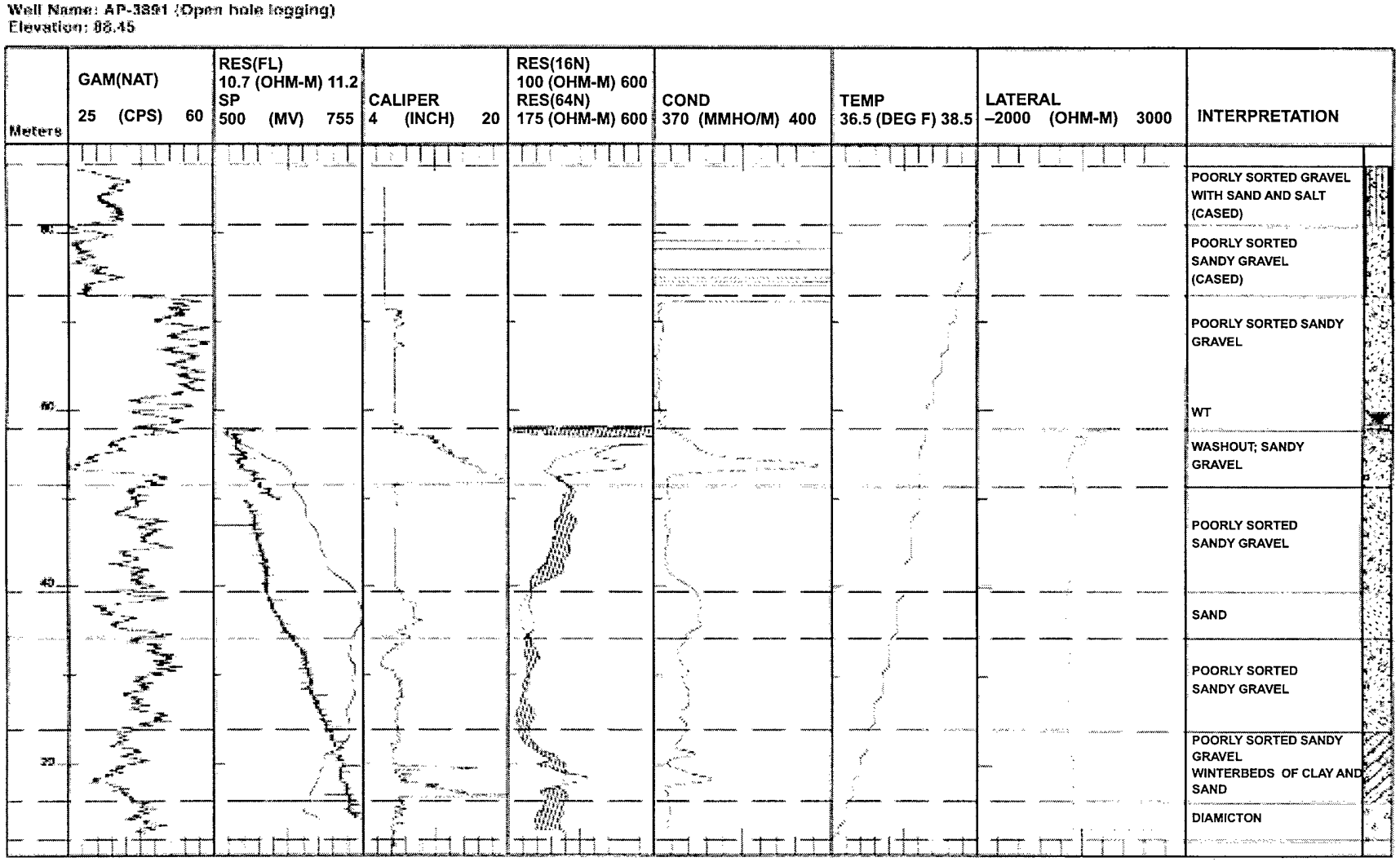


Figure 43. Open-hole logging of well AP-3891.

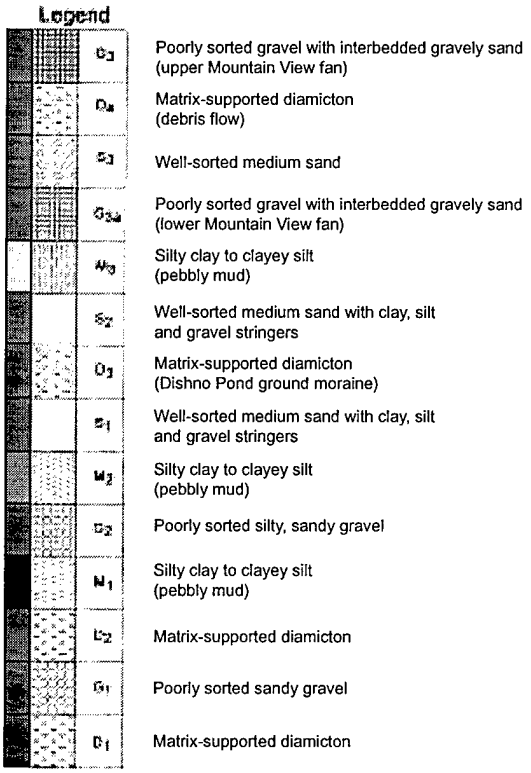


**Figure 44. Stratigraphic sequence below the Fort Richardson cantonment.**

a diamicton ($D_1$), which is found at the bottom of AP-3892 and AP-3903 (Fig. 46 and 49). This is a dense, matrix-supported diamicton with subangular to subrounded pebbles and granules suspended in a silty, sandy matrix (Table 4). In this unit, structure is generally lacking (i.e., massive) and clasts exhibit facets and striations. We interpret this diamicton as a subglacially deposited till (cf. Menzies and Shiltz 1996). It is overlain by a fluvial, poorly sorted, sandy gravel ($G_1$) that also occurs at the base of boreholes AP-3894, AP-3895, AP-3897, AP-3902, and AP-3909.

Overlying $G_1$ is a laterally discontinuous diamicton ($D_2$), which was encountered in AP-3892, AP-3894, AP-3895, AP-3902, and AP-3909 (Fig. 45 to 49). This diamicton is matrix supported, with a silty/sandy clay matrix, but it is generally not well compacted. Clasts have weak facets and some striations. We interpret this unit as a proximal debris flow deposit (cf., Lawson 1979, 1988, 1995) that is locally transitional at its upper contact with laminated silts (pebbly mud; $M_1$). It is encountered in boreholes AP-3894, AP-3895, AP-3902, and AP-3911. The thinly bedded mud is a silty clay to clayey silt with up to 11% gravel. Couplets, consisting of normally graded laminae with striated and facetted granules and pebbles, form outsized clasts. The mud unit appears to have been deposited during the marine transgression that accompanied glacial retreat. The

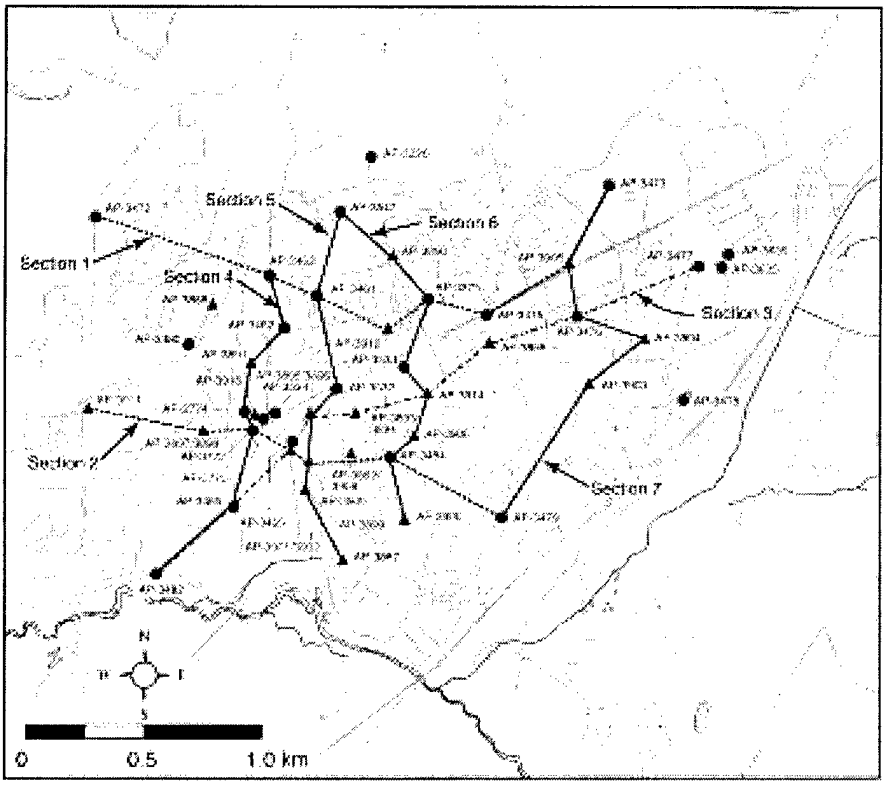


**Figure 45. Location of stratigraphic cross sections 1 to 7.**

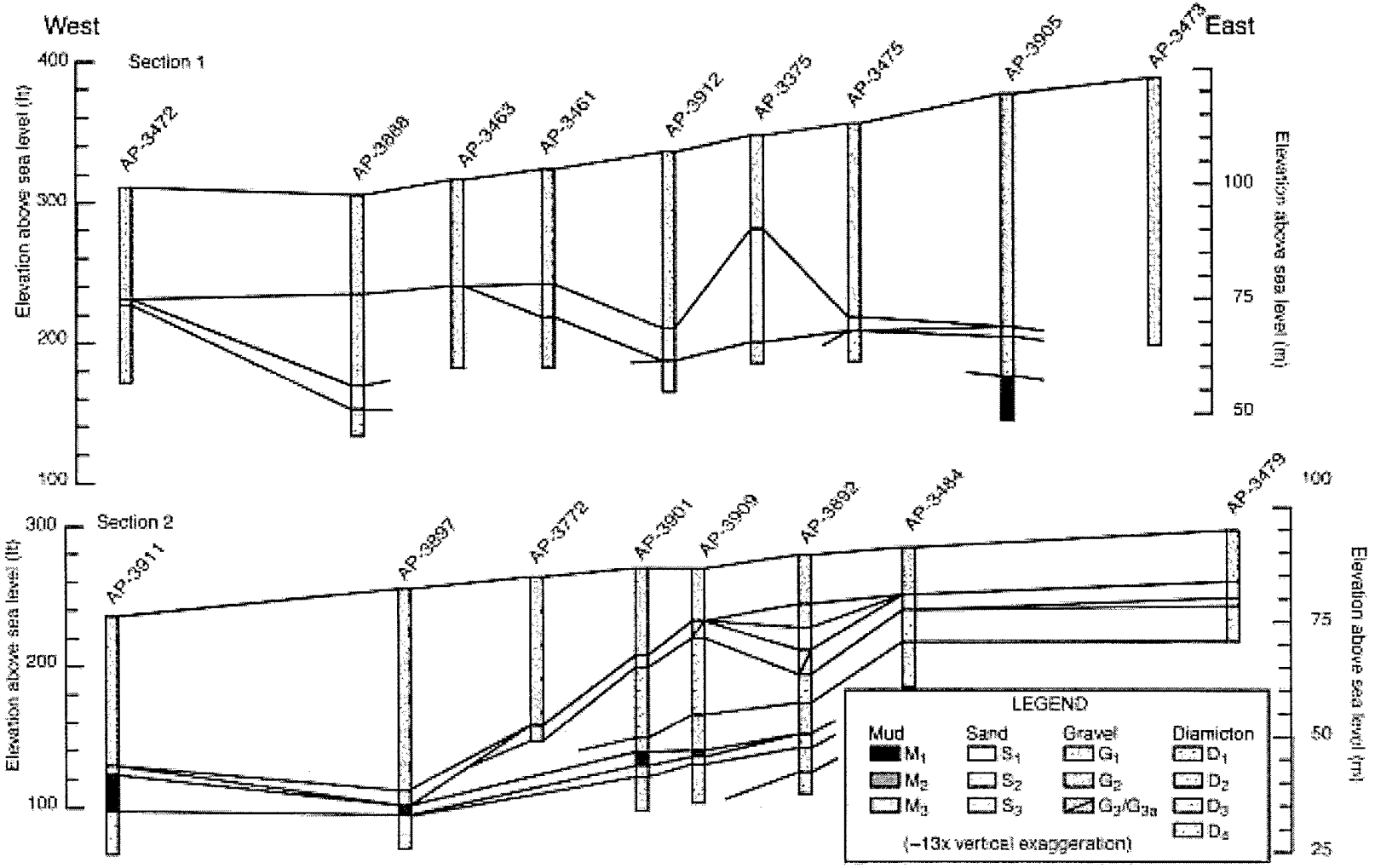


**Figure 46. Preliminary stratigraphic cross sections 1 and 2 showing geological relationships in the subsurface along east to west transects. Shading indicates potential confining layers.**

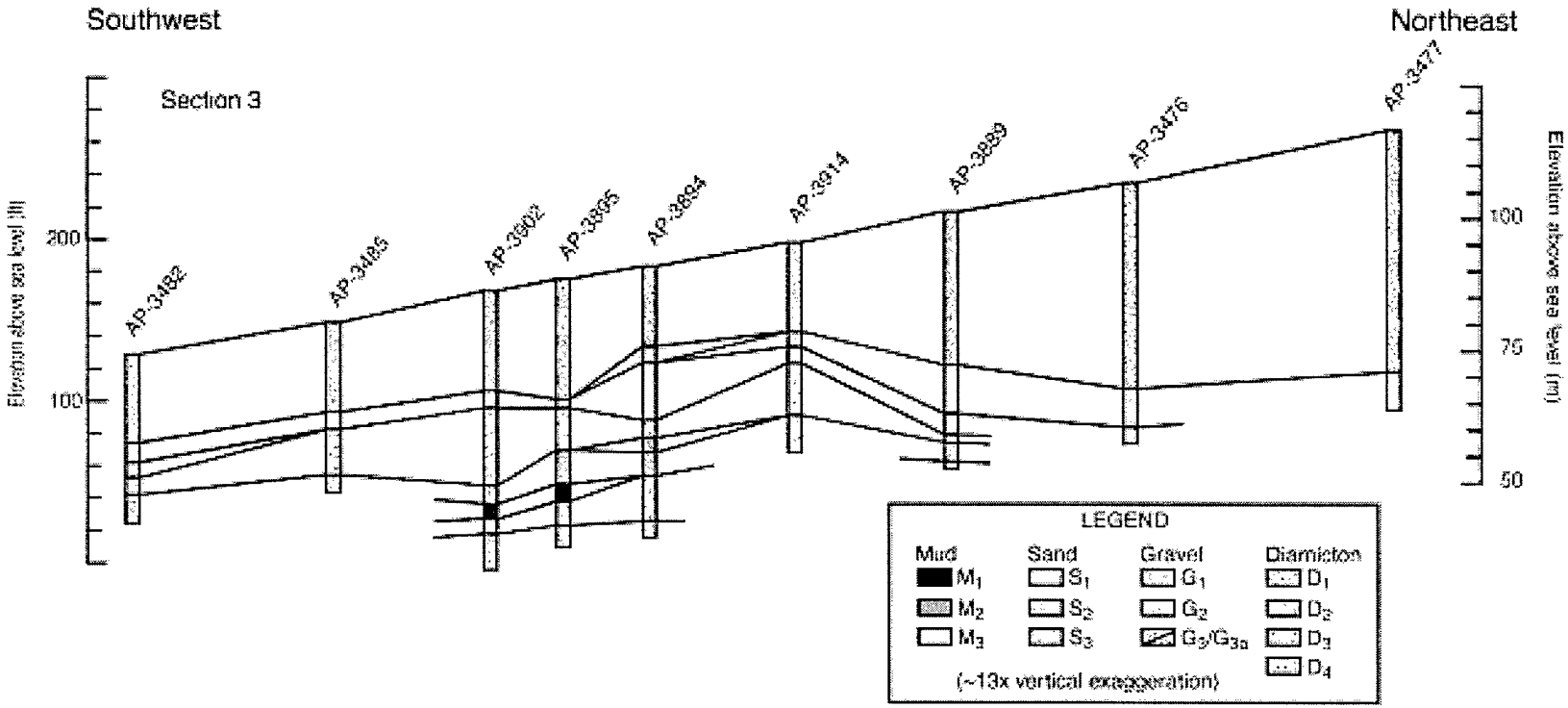


**Figure 47. Preliminary stratigraphic cross section 3 showing geological relationships in the subsurface along southwest to northeast transect. Shading indicates potential confining layers.**

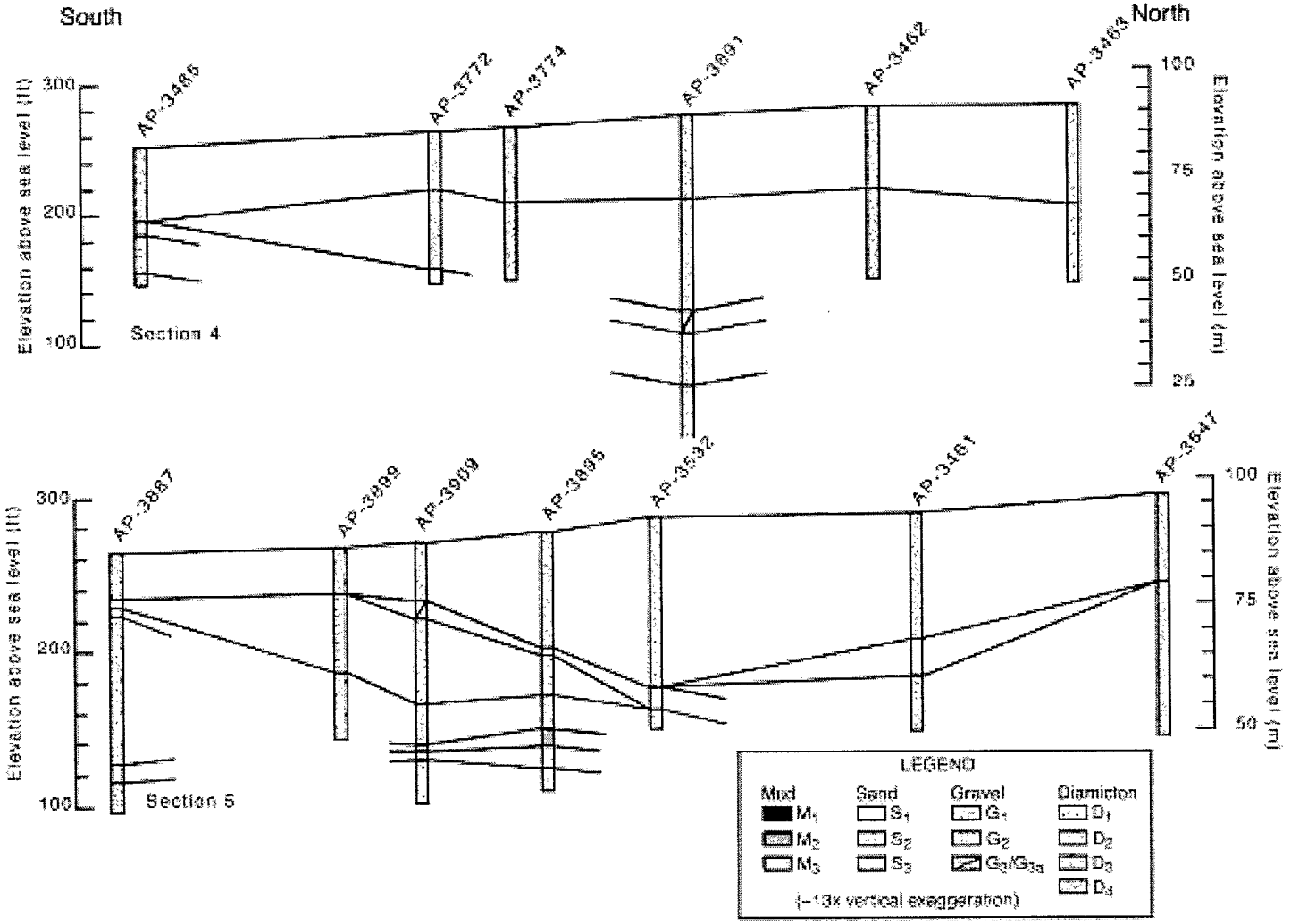


**Figure 48. Preliminary stratigraphic cross sections 4 and 5 showing geological relationships in the subsurface along south to north transects. Shading indicates potential confining layers.**

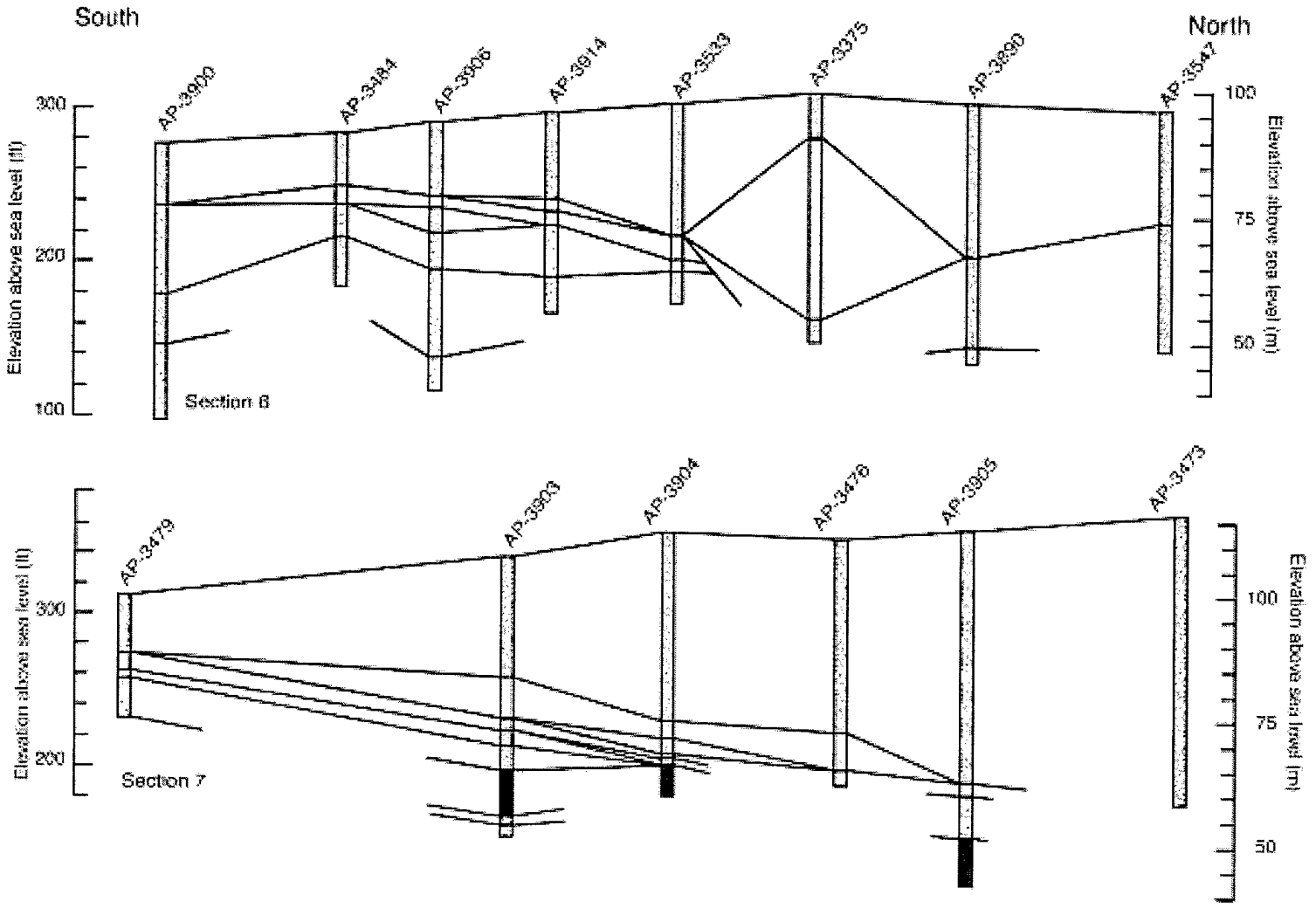


**Figure 49. Preliminary stratigraphic cross sections 6 and 7 showing geological relationships in the subsurface along south to north transects. Shading indicates potential confining layers.**

**Table 4. Summary of sedimentary units.**

| *Sedimentary unit* | *Description* |
|---|---|
| Sand | |
| $S_1$ | Well-sorted medium sand with localized silt, clay and gravel stringers. Locally show normally graded contact with overlying pebbly mud. |
| $S_2$ | Well-sorted medium sand with silt, clay and gravel stringers. Appears to be a gradation between diamicton ($D_3$) and mud ($M_3$). |
| $S_3$ | Thick, relatively extensive well-sorted medium sand that grades upward into laminated silt and fine sand. |
| Gravel | |
| $G_1$ | Poorly sorted sandy gravel. |
| $G_2$ | Poorly sorted silty sandy gravel. |
| $G_3/G_{3a}$ | Poorly sorted gravel with interbedded gravelly sand. |
| Pebbly mud | |
| $M_1$ | Silty clay to clay-rich silt with up to 11% gravel clasts; characterized by thin-bedded, normally graded couplets; clasts exhibit facets and striations. |
| $M_2$ | Silty clay to clay-rich silt with up to 22% gravel clasts; characterized by massive to thin-bedded, normally graded couplets; clasts exhibit facets and striations. Laterally extensive. |
| $M_3$ | Silty clay to clay-rich silt with up to 11% gravel clasts; laminated to thin bedded, normally graded couplets; clasts exhibit facets and striations. Laterally extensive. |
| Diamicton | |
| $D_1$ | Dense, matrix-supported with angular to subrounded particles and a silty sandy matrix. Generally massive, clasts facetted and striated. |
| $D_2$ | Discontinuous, matrix-supported, not overcompacted; weak facets and remnant striations on some clasts. |
| $D_3$ | Matrix-supported with 16 to 60% gravel clasts; middle of unit is overconsolidated with facetted, striated, and polished clasts; matrix is silty and locally clay-rich. Upper and lower contacts locally stratified. |
| $D_4$ | Matrix-supported with 22 to 26% clasts, 30 to 43% fines. Not overcompacted and may be locally stratified. |

outsized clasts were likely introduced through iceberg rafting and tell us that a calving tidewater glacier margin was nearby at the time (e.g., Hunter et al. 1996a, b; Cowan et al. 1996).

A second gravel ($G_2$) unit was encountered in 17 of the boreholes investigated. It is poorly sorted with a silty sandy matrix and is similar to the lowermost gravel unit ($G_1$; Table 4), which unconformably overlies mud ($M_1$; Fig. 46). At AP-3887 and AP-3894, the gravel is overlain by a second mud ($M_2$) that lies beneath a third diamicton ($D_3$; Fig. 47 and 48). This is a laminated silty mud ($M_2$), with thin, normally graded laminae and a few gravel clasts. It is classified as a pebbly mud. According to Mackiewicz et al. (1984) and Cowan and Powell (1990), such couplets are generated in the glacial-marine environment. Coarser particles are released from suspension at slack high tide. They then settle to the seafloor to form distinct layers that punctuate the near constant rainout of finer particles from suspension.

In the majority of monitoring wells that encountered gravel $G_2$, it is overlain by a prominent, matrix-supported diamicton ($D_3$; AP-3484, AP-3485, AP-3533, AP-3889, AP-3892, AP-3899, AP-3900, AP-3902, AP-3903, AP-3906, AP-3909, and AP-3914) (Fig. 46–49). This diamicton contains 16 to 60% gravel clasts, many of which are facetted, striated, and polished. The matrix is silt- to clay-rich and generally overconsolidated in the center of the unit. However, at the upper and lower boundaries, the matrix is often sandier and locally stratified. We interpret this unit as a subglacial lodgement deposit that is bracketed by debris flow and meltout deposits. Diamicton ($D_3$) is spatially restricted to the southwest portion of the cantonment area and extends northeasterly to AP-3905 (Fig. 50).

Sand ($S_2$) was encountered above the diamicton ($D_3$) in AP-3479, AP-3892, and AP-3906 (Table 4; Fig. 46 and 49). The sand is well-sorted and medium in size, with a few silt, clay, and gravel stringers, and is overlain by a third mud horizon ($M_3$). The sand may be a

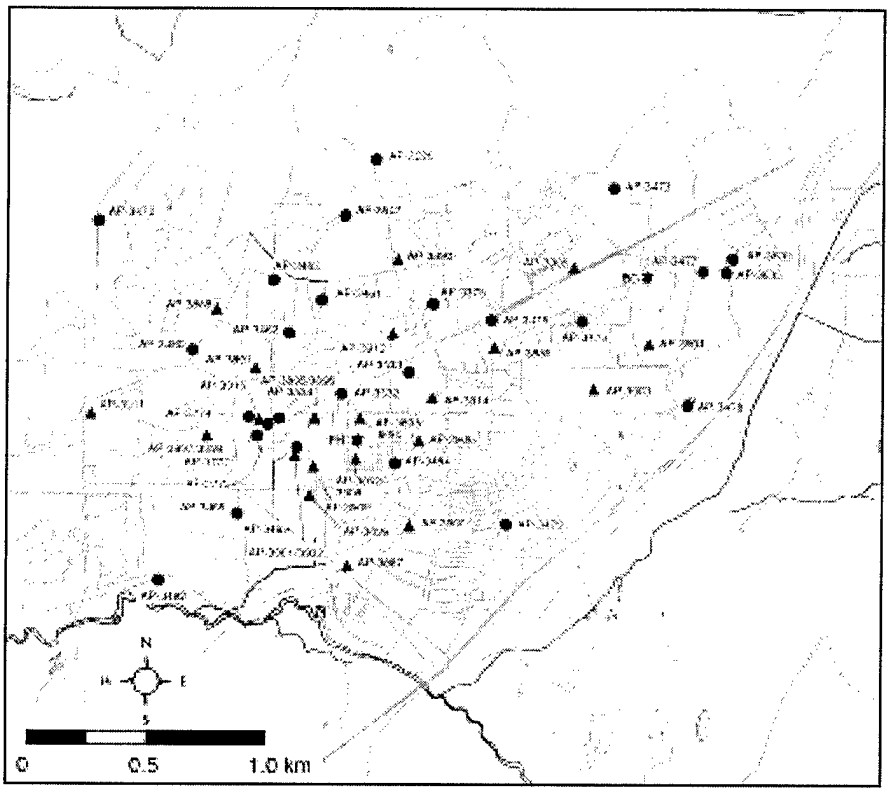


**Figure 50. Occurrence of diamicton $D_3$ as defined by borehole samples and geophysical logging.**

gradational phase between the diamicton ($D_3$) and the mud ($M_3$). Since continuous cores are not available, the nature of the contact and origin of the sediments cannot be described.

The third mud unit ($M_3$) is common in the middle of the stratigraphic column in many of the boreholes near the center of the cantonment (Fig. 46–49, 51). This mud is laminated to thinly bedded, and generally consists of a silty clay to clay-rich silt with up to 11% gravel. Laminae couplets are normally graded, with striated and facetted granules and pebbles forming outsized clasts. This unit appears to be a pebbly mud deposited in a shallow estuarine environment during the marine transgression that accompanied the final period of glacial retreat.

A thick sand unit ($S_3$) was encountered above the pebbly mud ($M_3$) and an uppermost diamicton ($D_4$); however, locally (at 50 m depth, AP-3897) the sand appears to overlie the lower pebbly mud ($M_1$), indicating deep erosion and removal of the layers that are normally below it. The sand is locally (AP-3461, AP-3375) sandwiched between two sandy gravels; it may be a lateral equivalent to a sandy zone within stratified sandy gravel/gravelly sand that is found in AP-3461, AP-3462, AP-3463, AP-3473, AP-3475, and AP-3905. The lower gravel ($G_{3a}$) appears to have been deposited as an early stage of the Mountain View fan (Fig. 46 and 48). The base of the sand may be gradational with pebbly mud ($M_3$), suggesting that the marine environment was becoming more shallow or perhaps that the outwash deposition from the ice margin extended into this area (e.g., AP-3889). This and other similar zones with high sand content can be followed laterally in the geophysical logs.

The uppermost diamicton ($D_4$) was found only in monitoring wells AP-3892 and AP-3894 and is not laterally continuous (Fig. 46 and 47). This diamicton is matrix-supported with a silty-sandy matrix that is not well compacted. It contains 30 to 43% fines and 22 to 26% gravel with some clasts showing facets and striations. We interpret the unit as a debris flow deposit, whose source may have been an older diamicton in the glacially streamlined hill to the south (Birch Hill; cf. Lawson 1979, 1988).

The uppermost gravel ($G_3$) has the greatest volume in the cantonment area (Fig. 46–49). It is texturally complex, consisting of poorly sorted gravel with a matrix composition that varies vertically. It may be interbedded with gravelly sand. This gravel may be up to 46 to 49 m thick (AP-3897, AP-3477) and is

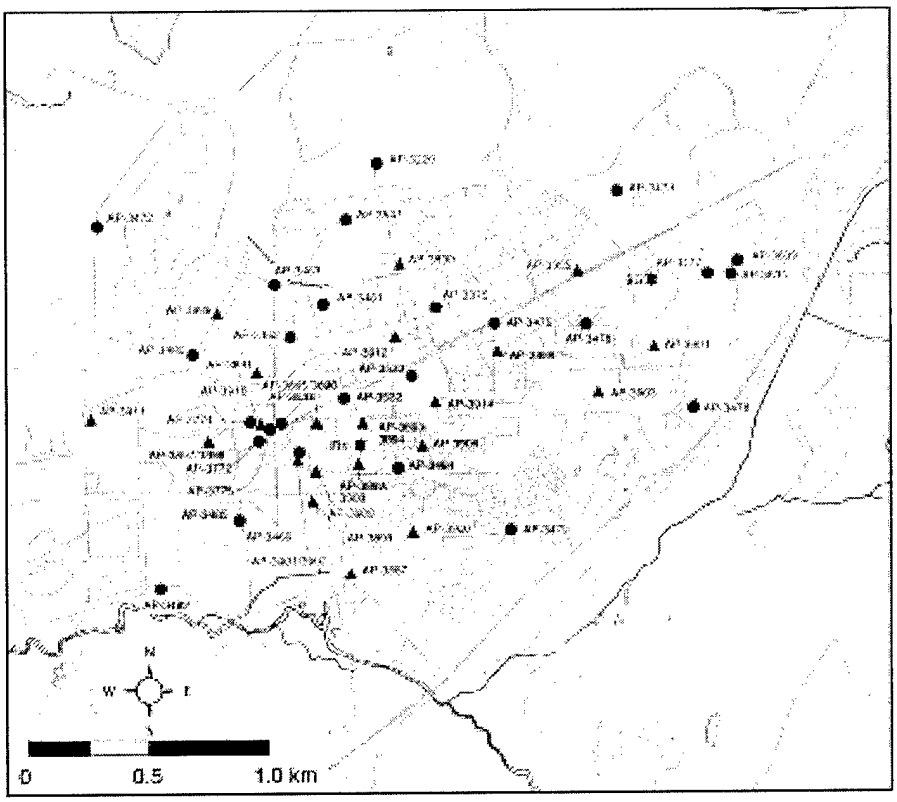


**Figure 51. Occurrence of pebbly mud $M_3$ as defined by borehole samples and geophysical logging.**

interpreted as outwash deposits of the Mountain View fan.

## CONCEPTUAL MODEL OF SUBSURFACE STRATIGRAPHY AND GEOLOGY

The spatial relationships among the 14 sedimentary units are shown in seven geological cross sections of the cantonment area (Fig. 45 to 49). The cross sections trend generally west to east (sections 1 and 2), southwest to northeast (section 3), and south to north (sections 4 to 7; Fig. 45).

### Cross section 1

Cross section 1, located just south of the Elmendorf Moraine, consists of a gravel unit ($G_3$) that thins from east (58 m, AP-3473) to west (about 23 m, AP-3888) and is underlain by sand ($S_3$) in the middle of the section. This sand pinches out to the west, where it overlies a lower gravel unit ($G_{3a}$). Diamicton ($D_3$) was encountered at elevations of 69 and 57 m in AP-3475 and AP-3905, respectively. A pebbly mud ($M_3$) encountered in AP-3472, AP-3888, and AP-3905 apparently underlies $G_3$ and $G_{3a}$ across most of the area. Boreholes AP-3463, AP-3461, AP-3375, and AP-3473 were not drilled deep enough to encounter the underlying confining layers (either $D_3$ or $M_3$). The absence of the pebbly mud ($M_3$) at AP-3475 likely represents local erosion and incision into diamicton ($D_3$) at the base of the sand ($S_3$).

### Cross section 2

At the northeast end of cross section 2, gravel ($G_3$) is approximately 13 m thick, but then thickens dramatically to 43.6 m towards the western end (Fig. 46). In the east, the top surface of the pebbly mud ($M_3$) and diamicton ($D_3$) rises to form an apparent plateau or buried topographic high. This corresponds with the shallow resistive layer found below the cantonment area (Fig. 5). In the core of this feature, deeper pebbly mud ($M_1$ and $M_2$) and diamicton ($D_1$ and $D_2$) horizons are interbedded with sand ($S_2$ and $S_3$) and gravel ($G_1$ and $G_2$). The sandy nature of the pebbly mud ($M_3$) at several locations tells us that it was close to the sediment source and potentially modified by waves in a shallow, near-shore location. The pebbly mud and diamicton dip steeply to the west between AP-3909 and AP-3772, but they pinch out before AP-3897.

The pebbly mud is likely an estuarine sediment deposited in a shallow bay north of the buried plateau

and may be the northern extent of the Bootlegger Cove Formation (Miller and Dobrovolny 1959). Modern process studies show that such pebbly muds are deposited through suspension settling of fine particles transported in turbid fresh water layers (Mackiewicz et al. 1984, Cowan and Powell 1990, Powell and Domack 1995, Hunter et al. 1996a, b). The settling of these fine particles forms a blanket deposit that drapes over existing surfaces. The coarse particles and gravel clasts are introduced through iceberg rafting and release as the icebergs melt, break, and roll (e.g., Ovenshine 1970, Thomas and Connell 1985, Cowan et al. 1996). Therefore, the dipping surface of the pebbly mud is a primary feature formed as sediment deposited on the surface of the lower diamicton unit $D_3$. Diamicton unit $D_3$ is probably equivalent to the Dishno Pond ground moraine mapped by Yehle and Schmoll (1987a, b, 1989), Yehle et al. (1990, 1992) and Schmoll et al. (1996). We interpret the absence of the pebbly mud ($M_3$) and diamicton ($D_3$) at AP-3897 to reflect deep erosion and scour by a proglacial stream that either preceded or accompanied early phases of the Mountain View fan formation. The upper diamicton ($D_3$) occurs in AP-3911, south of this area of intense scour.

This interpretation suggests that the upper confining layer may be breached for an unknown distance between AP-3772 and AP-3911. Therefore, there is a strong possibility that the upper unconfined and lower confined aquifers are hydraulically connected. Communication with deeper aquifers is, however, probably restricted by the lower pebbly mud ($M_1$) and diamicton ($D_2$) horizons encountered at AP-3892, AP-3909, AP-3902, AP-3897, and AP-3911. There are at least two deeper confined aquifers that may be hydraulically connected. Additional deep boreholes and ground water analyses are required to determine if this is true beneath the cantonment area. This is consistent with the findings of Cederstrom et al. (1964).

### Cross section 3

Cross section 3 trends approximately southwest to northeast across the center of the cantonment (Fig. 47). Gravel unit ($G_3$) is thickest to the northeast at AP-3477, the borehole nearest the apex of the fan and mouth of the Eagle River Valley. In the northeast section, there is a sand ($S_3$; Fig. 52) at the base of gravel unit ($G_3$). As gravel unit ($G_3$) thins to the southwest, the sand ($S_3$) pinches out on the flanks of the subsurface high in the pebbly mud ($M_3$) and diamicton ($D_3$) shown on cross section 2 (Fig. 45). The pebbly mud and diamicton units apparently form a continuous confining horizon along cross section 3 (Fig. 47). These units are thickest between AP-3485 to the southwest and AP-3914 in the center of the cantonment (Fig. 3 and 45).

### Cross sections 4–7

In cross sections 4 through 7, gravel unit ($G_3$) thickens to the north (Fig. 48 and 49). A sand horizon ($S_3$) in sections 5 to 7 forms a lens below the middle of the cantonment. At AP-3375, AP-3461, and AP-3904, the sand overlies a second, coarser gravel ($G_{3a}$). The contact between gravel ($G_3$) and sand ($S_3$), and the patterns of the geophysical response to gravel ($G_{3a}$), can be traced laterally across the entire area. Where sand ($S_3$) pinches out, the contact between ($G_3$) and ($G_{3a}$) can similarly be identified (section 4) (Fig. 48). The base of the sand ($S_3$) is apparently erosional; it was probably deposited when the Mountain View fan formed. The sand is also restricted to the northern flank of the pebbly mud ($M_3$) and diamicton ($D_3$) plateau, and extends north, midway between AP-3912–AP-3890 and AP-3475–AP-3905 (Fig. 52). North of here, gravel unit ($G_3$) is deeply incised, truncating unit $S_3$.

Between AP-3533 and AP-3375 (section 6), the base of gravel ($G_{3a}$) is apparently erosional and units $M_3$ and $D_3$ have been truncated (Fig. 49). This erosion does not appear to penetrate into the deeper underlying diamicton ($D_2$); however, the upper gravels in the confined aquifer can likely communicate with the unconfined aquifer in this region. South of the truncation of mud ($M_3$) and diamicton ($D_3$) in the southern parts of sections 5 and 6, these layers dip more steeply than on sections 4 and 7 (Fig. 48 and 49).

The buried plateau defined by the surface of pebbly mud ($M_3$) and diamicton ($D_3$) is well demonstrated in cross sections 3–7 (Fig. 47–49). This feature is a buried landform, probably a drumlin, similar to those located south of the Mountain View fan (Schmoll et al. 1996, Hunter et al. 1997c). It appears to extend through the gravel horizon and reaches the surface in the form of Birch Hill. If this is the case, the pebbly mud ($M_3$) that drapes over the lower diamicton (Dishno Pond; $D_3$) is absent on the hill, probably because of erosion by waves. In AP-3909, the pebbly mud is transitional to a sand and is good evidence that such winnowing and erosion took place (Fig. 48). The sand would then be a beach or near-shore deposit. Other areas of the cantonment where topographic features are buried (e.g., AP-3899) would similarly be devoid of this mud.

### Synthesis

The stratified sand and gravel of unit ($G_3$) and its sub-units represent stacked cut-and-fill sequences formed by a sediment-laden proglacial stream that was rapidly migrating (Gurnell and Clark 1987, Lawson 1993, 1995). The normal patterns of braided stream migration and deposition (e.g., Jopling and McDonald 1975, Smith 1970, 1985) are periodically punctuated by incision and subsequent rapid deposition of sedi-

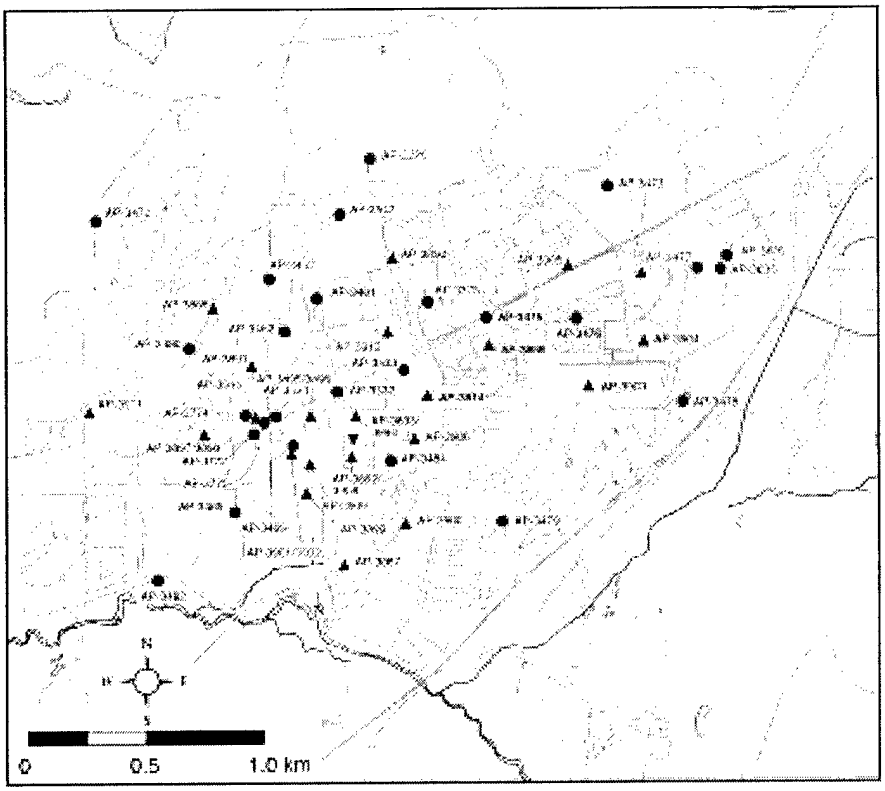


**Figure 52. Occurrence of sand $S_3$ as defined by borehole samples and geophysical logging.**

ment during each catastrophic lake discharge from the Eagle River Valley (Schmoll et al. 1996). These processes have caused the discontinuities in the fine- and coarse-grained strata that produce the complex ground water conditions. The lateral extent and stratigraphic equivalence of the lowermost sand, gravel, pebbly mud, and diamicton units are difficult to interpret because not enough deep boreholes encounter them.

The unconfined aquifer is present in the upper sand ($S_3$) and gravel ($G_3$) units that generally overlie the fine-grained units $M_3$ and $D_3$, which confine another aquifer in the underlying sand and gravels. The basal surface contours of the unconfined aquifer (units $G_3$, $G_{3a}$ and $S_3$; Fig. 53) roughly represent the base of the Mountain View fan. The buried-topographic high of the pebbly mud–diamicton plateau is apparent in the southeast. In contrast, there is a trough between the plateau and the southern margin of the Elmendorf Moraine. This trough points to fluvial processes that were active in front of the Elmendorf ice as it advanced, causing erosion of the older pebbly mud ($M_3$) and diamicton ($D_3$) units. This basin was subsequently filled with outwash sediments from the catastrophic discharges of lakes in the Eagle River Valley.

Ground water flow patterns described by Hunter et al. (2000) reflect this three-dimensional stratigraphic architecture. Seasonal ground water data collected by the U.S. Army Engineer District, Alaska (USACE 1996), show descending water levels to the west and north of the main cantonment. These water levels roughly coincide with the slopes of the buried surface topography of the pebbly mud–diamicton units (Fig. 46 to 49, 53, 54). The effect of this subsurface geometry on aquifers is amplified during November, when they recharge and water levels are low. At this time, regional ground water flow patterns are deflected by the local subsurface topography. During the summer, ground water flows to the west in the northern portion of the cantonment (Fig. 54), but in November flow is locally diverted. For example, near AP-3375, ground water moves around the high point in the confining layer surface (Fig. 53).

Ground water flow in the confined aquifer is more regular and has a gentle, northwest-sloping potentiometric surface. Ground water in this aquifer is fed by recharge along the flanks of the Chugach Mountains. Hunter et al. (2000) compared the potentiometric surfaces defined by Cederstrom et al. (1964) and USACE (1996), finding these data to be consistent despite the three-decade interval between the measurements.

The complexity of flow within the confined aquifer

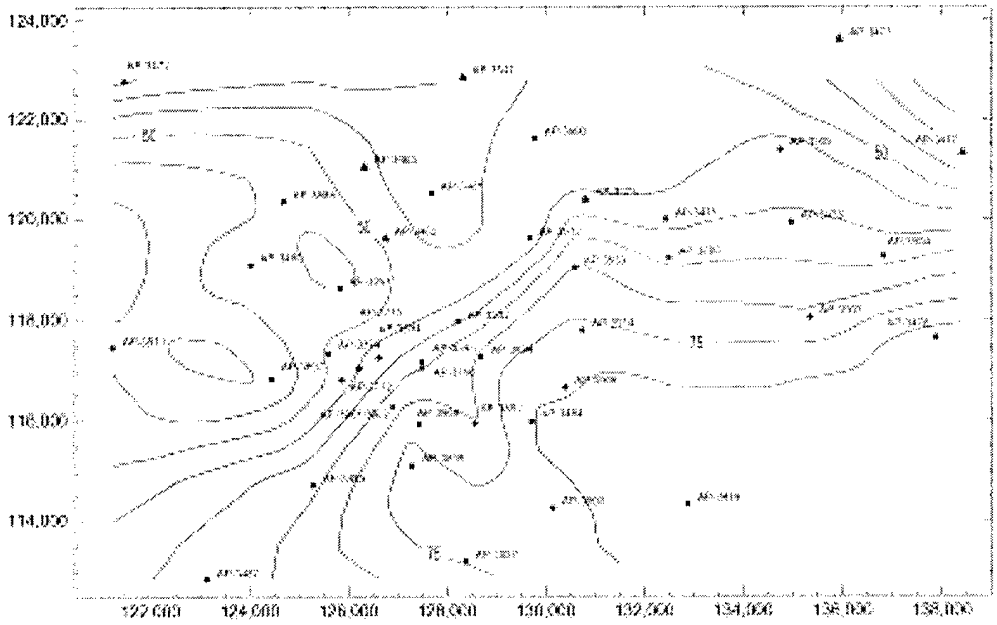


**Figure 53. Elevation (m) at the top of the confining layer ($D_3$ and $M_3$) below the Fort Richardson cantonment. Circles indicate boreholes that encountered the confining layer. Triangles indicate boreholes that penetrated only the upper aquifer.**

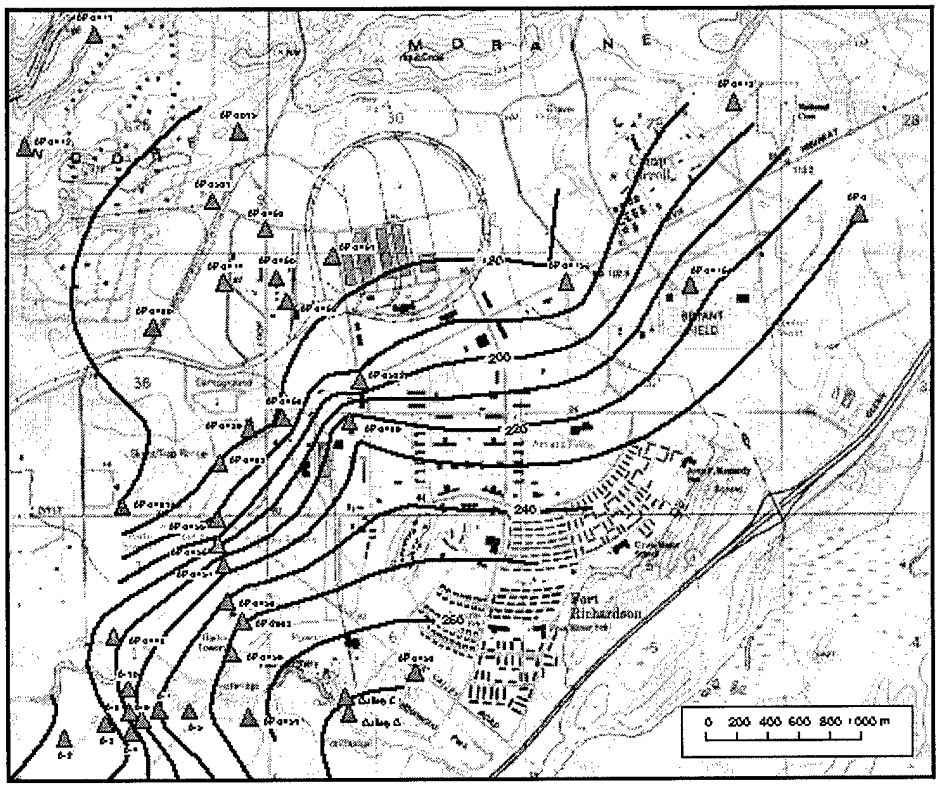


a. Confined aquifer—May 1995.

**Figure 54. Ground water levels. (After USACE 1996.)**

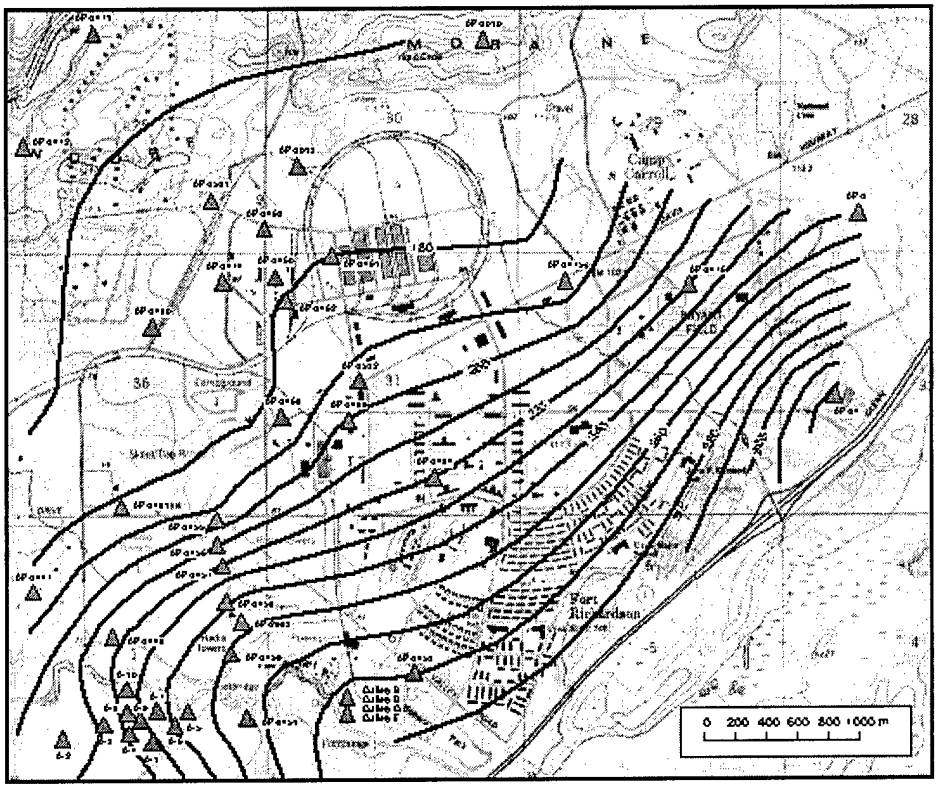


b. Unconfined aquifer—August 1995.

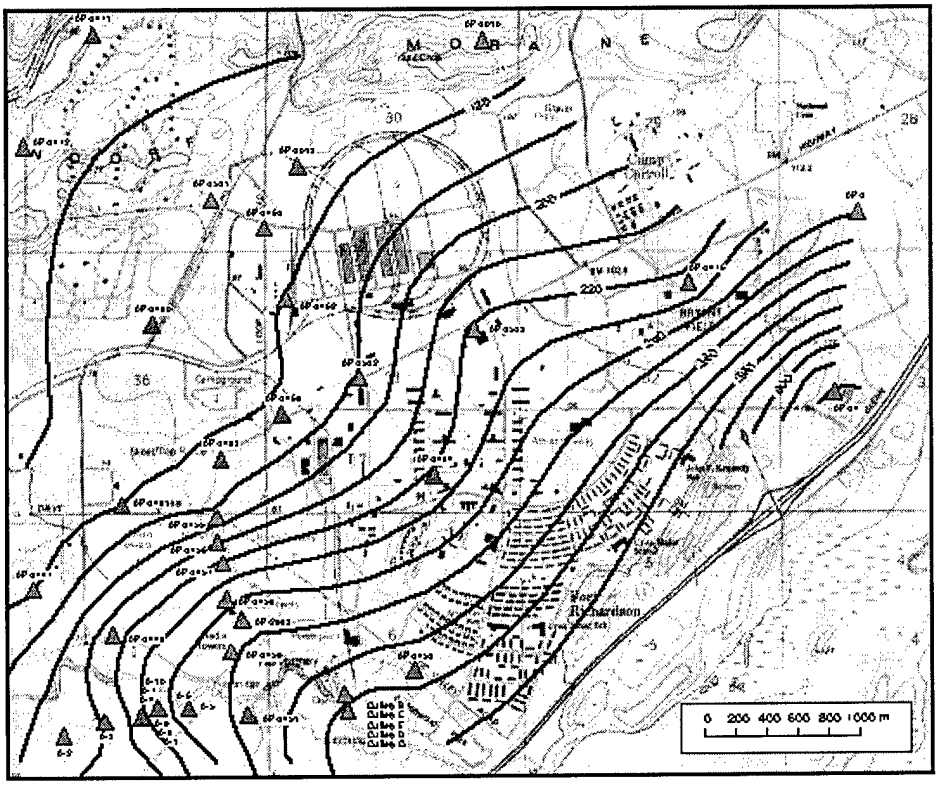


c. Unconfined aquifer—November 1996.

Figure 54 *(cont'd)*.

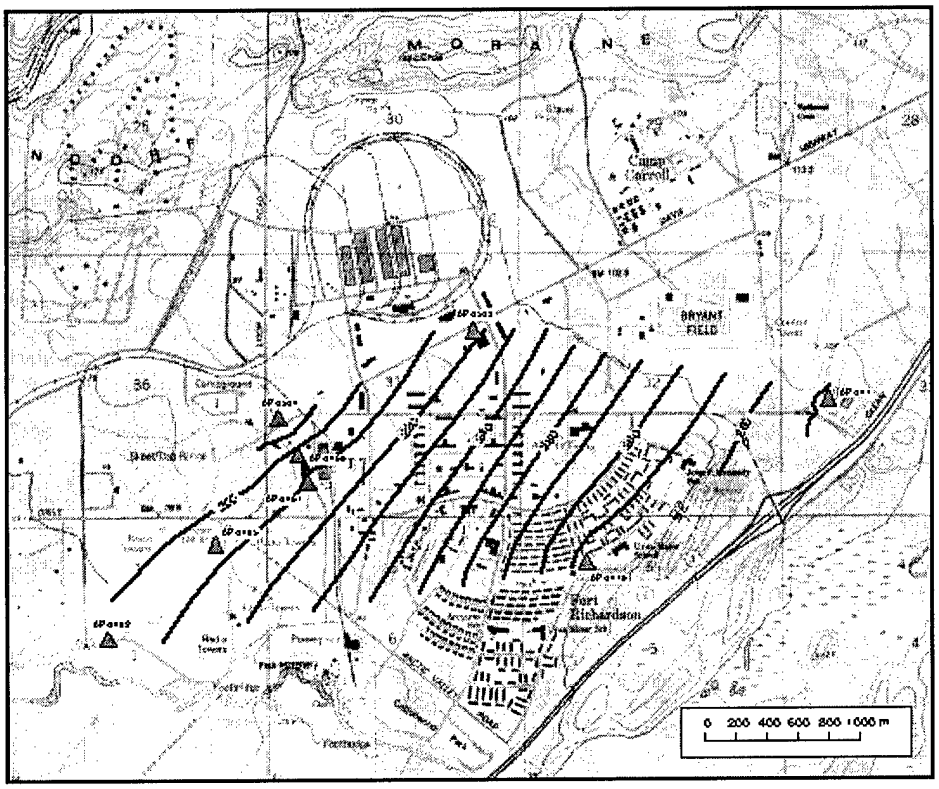


d. Confined aquifer—May 1995.

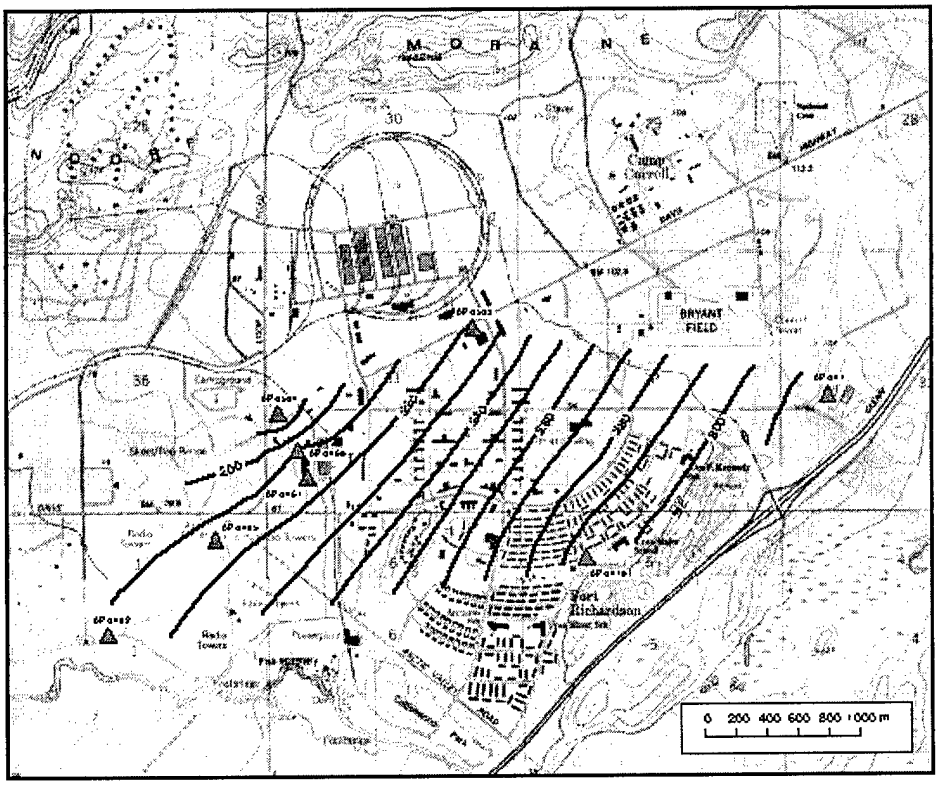


e. Confined aquifer—August 1995.

**Figure 54 *(cont'd).* Ground water levels. (After USACE 1996.)**

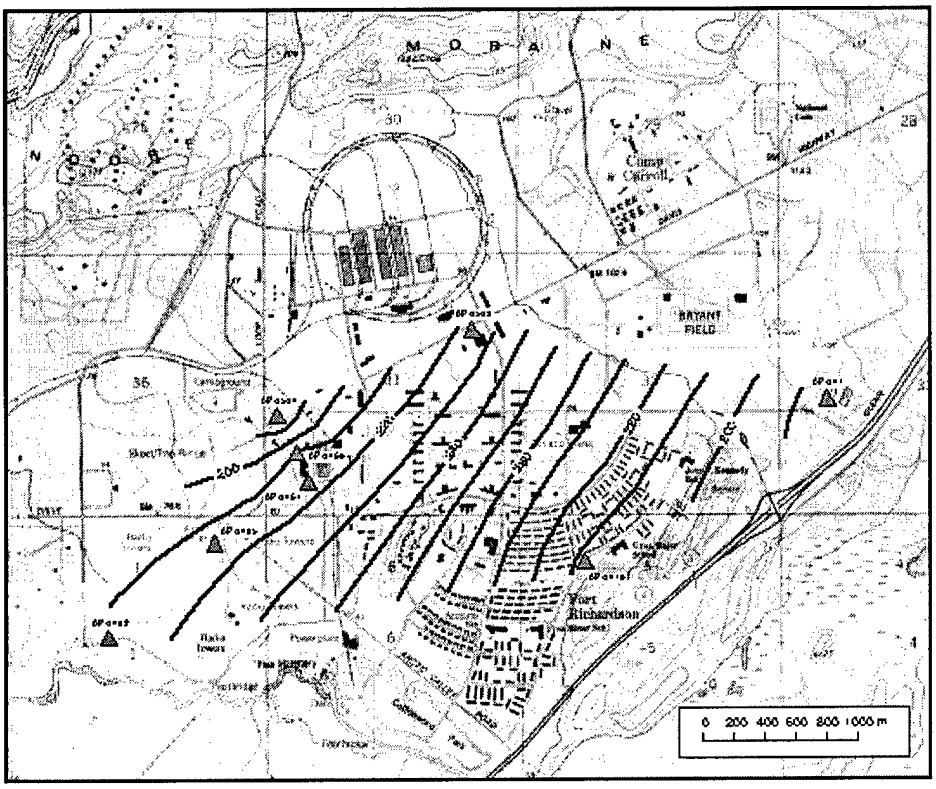


**f. Confined aquifer—November 1995.**

**Figure 54 *(cont'd).***

cannot be evaluated from these data. Our stratigraphic interpretations tell us that the deeper confining layers ($D_2$, $D_1$, $M_2$, $M_1$) are laterally extensive and undissected below the cantonment area; however, they do appear to be truncated just north of the cantonment and south of the Elmendorf Moraine. If this is the case, local communication of ground water through vertical flow is unlikely except near the Elmendorf Moraine, and each of the buried sand and gravel units make up a locally confined aquifer.

## CONCLUSIONS

The sediments below Fort Richardson originated during Late Wisconsinan glaciation of the Anchorage basin. Clay, silt, sand, gravel, and diamicton stratigraphic units were deposited during multiple advances and retreats in the glacier margin. At least three diamicton units were deposited in the cantonment area as a result of these oscillations in the glacier margin. These diamictons were deposited either directly from the glacier, subglacially as a lodgement till, or by subaerial or submarine debris flows from the glacier margin. The diamictons are closely associated with two pebbly mud horizons, which are laminated with few clasts; laterally, they grade to silt and clay layers. The pebbly muds apparently were deposited in shallow estuaries or in deeper water, where iceberg rafting in front of tidewater glacier margins introduced the gravel clasts. We have insufficient data to define which origin is correct. The diamicton and pebbly mud layers are interbedded with sand and gravel horizons; these latter horizons contain ground water while the diamictons and muds act as confining layers for these aquifers.

Sand and gravel layers are highly variable in thickness and extent. The most pronounced of these is the upper silty, sandy gravel of the Mountain View fan, which extends to more than 60 m depth under the cantonment. This gravel generally overlies the pebbly mud and diamicton horizons. The upper gravel locally truncates the mud and diamicton confining horizon, which means that the confined and unconfined aquifers below this horizon can communicate with one another. However, the borehole and downhole geophysical data are insufficient to fully define where this happens. The extent of the lowermost diamicton, which confines a second lower aquifer ($G_2$), is also poorly defined.

Our stratigraphic observations explain the existing, but limited, ground water data. Ground water in the

unconfined aquifer generally flows to the north and west towards a trough below the Mountain View fan. The flow patterns change when water levels are low as the ground water flows around topographic highs on the surface of the underlying diamicton and mud.

Ground water in the confined aquifer beneath this diamicton follows the potentiometric surface, which presumably means that it recharges from the Chugach Mountains. Ground water flows generally northwesterly, but the unconfined and confined aquifers become a single aquifer where the mud–diamicton unit is truncated along the northern and western areas of the cantonment.

## LITERATURE CITED


**Astley, B.N., D.E. Lawson, C. Snyder, A.J. Delaney, S.A. Arcone, and L.E. Hunter** (1999) Stratigraphic, aquifer distribution and potential contaminant migration pathways based on ground resistivity and GPR analyses, Water Treatment Plant, Fort Richardson, AK. U.S. Army Cold Regions Research and Engineering Laboratory. (CRREL Contract Report to U.S. Army, Alaska, Directorate of Public Works.)

**Asquith, G., and C. Gibson** (1982) *Basic Well Log Analysis for Geologists*. Tulsa, Oklahoma: The American Association of Petroleum Geologists.

**ASTM** (1995) Standard practice for description and identification of soils (visual-manual procedure), D2488-93. In *1995 Annual Book of ASTM Standards*. West Conshocken, Pennsylvania: American Society for Testing and Materials, p. 218–228.

**Cederstrom, D.J., F.W. Trainer, and R.M. Waller** (1964) Geology and ground-water resources of the Anchorage Area, Alaska. Washington, D.C.: U.S. Geological Survey, Water-Supply Paper 1773.

**Conlog** (1990) Comparison of induction logs with electric logs. *Technical Notes*, **1**(3): 3.

**Cowan, E.A., P.R. Carlson, and R.D. Powell** (1996) The marine record of the Russell Fiord outburst flood, Alaska, U.S.A. *Annals of Glaciology*, **22**: 194–199.

**Cowan, E.A., and R.D. Powell** (1990) Suspended sediment transport and deposition of cyclically interlaminated sediment in a temperate glacial fjord, Alaska, U.S.A. In *Glacimarine Environments: Processes and Sediments* (J.A. Dowdeswell and J.D. Scourse, Eds.). London: Geological Society of London, Special Publication 53, p. 75–90.

**Dowdeswell, J.A., and E.K. Dowdeswell** (1989) Debris in icebergs and rate of glaci-marine sedimentation: Observations from Spitsbergen and a simple model. *Journal of Geology*, **97**: 221–231.

**Gilbert, R.** (1990) Rafting in glacimarine environments. In *Glacimarine Environments: Processes and Sediments* (J.A. Dowdeswell and J.D. Scources, Eds.), p. 105–120.

**Gurnell, A.M., and J.C. Clark** (1987) *Glacio-fluvial Sediment Transfer*. New York: John Wiley and Sons.

**Hunter, L.E., R.D. Powell, and D.E. Lawson** (1996a) Morainal-bank sediment budgets and their influence on the stability of tidewater termini of valley glaciers entering Glacier Bay, Alaska, U.S.A. *Annals of Glaciology*, **22**: 211–216.

**Hunter, L.E., R.D. Powell, and G.W. Smith** (1996b) Facies architecture and grounding-line fan processes of morainal banks during deglaciation of coastal Maine. *Geological Society of America Bulletin*, **108**(8): 1022–1038.

**Hunter, L.E., S.A. Arcone, A.J. Delaney, and D.E. Lawson** (1997a) Feasibility of using resistivity geophysical surveys for mapping the confining layer on Fort Richardson: Preliminary results. U.S. Army Cold Regions Research and Engineering Laboratory. (CRREL Contract Report to U.S. Army, Alaska, Directorate of Public Works.)

**Hunter, L.E., D.E. Lawson, S.R. Bigl, and J.C. Strasser** (1997b) Endnote Plus bibliographic database on Fort Richardson, Alaska, geology and hydrogeology. U.S. Army Cold Regions Research and Engineering Laboratory. (CRREL Contract Report to U.S. Army, Alaska, Directorate of Public Works.)

**Hunter, L.E., D.E. Lawson, S.R. Bigl, J.D. Schlagel, and J.C. Strasser** (1997c) The glacial geology and stratigraphy of Fort Richardson: A synthesis of the hydrogeologic framework, Interim draft report. U.S. Army Cold Regions Research and Engineering Laboratory. (CRREL Contract Report to U.S. Army, Alaska, Directorate of Public Works.)

**Hunter, L.E., D.E. Lawson, S.R. Bigl, B.N. Astley, C. Snyder, and F. Perron** (1999) Subsurface geologic investigations of the Fort Richardson cantonment, AK. U.S. Army Cold Regions Research and Engineering Laboratory. (CRREL Contract Report to U.S. Army, Alaska, Directorate of Public Works.)

**Hunter, L.E., D.E. Lawson, S.R. Bigl, and J.D. Schlagel** (2000) Glacial geology and stratigraphy of Fort Richardson: A review of available data on the hydrogeology. U.S. Army Engineer Research and Development Center, Cold Regions Research and Engineering Laboratory, TR-00-03.

**Jackson, J.A., Ed.** (1997) *Glossary of Geology*. Alexandria, Virginia: American Geological Institute.

**Jopling, A.V. , and B.C. McDonald, Eds.** (1975) *Glaciofluvial and Glaciolacustrine Sedimentation*. Tulsa, Oklahoma: Society of Economic Paleontologists and Mineralogists, Special Publication 23.

**Karlstrom, T.N.V.** (1964) Quaternary geology of the

Kenai Lowland and glacial history of the Cook Inlet region, Alaska. Washington, D.C.: U.S. Geological Survey Professional Paper 443.

**Keys, W.S., and L.M. MacCary** (1971) Applications of borehole geophysics to water-resources investigations. Alexandria, Virginia: U.S. Geological Survey, Book 2, Chapter E1.

**Lawson, D.E.** (1979) Sedimentological analysis of the western terminus region of the Matanuska Glacier, Alaska. U.S. Army Cold Regions Research and Engineering Laboratory, CRREL Report 79-9.

**Lawson, D.E.** (1988) Glacigenic resedimentation: Classification concepts and application to mass-movement processes and deposits. In *Genetic Classification of Glacigenic Deposits* (R.P. Goldthwait and C.L. Matsch, Eds.). Rotterdam: Balkema, p. 147–172.

**Lawson, D.E.** (1993) Glaciohydrologic and glaciohydraulic effects on runoff and sediment yield in glacierized basins. U.S. Army Cold Region Research and Engineering Laboratory, Monograph 93-2.

**Lawson, D.E.** (1995) Sedimentary and hydrologic processes within modern terrestrial valley glaciers. In *Modern Glacial Environments: Processes, Dynamics, and Sediments* (J. Menzies, Ed.). Boston, Massachusetts: Butterworth-Heinemann, Ltd., p. 337–363.

**Mackiewicz, N.E., R.D. Powell, P.R. Carlson, and B.F. Molnia** (1984) Interlaminated ice-proximal glacimarine sediment in Muir Inlet, Alaska. *Marine Geology*, **57**: 113–147.

**Menzies, J., and W.W. Shiltz** (1996) Subglacial environments. In *Past Glacial Environments: Sediments, Forms and Techniques* (J. Menzies, Ed.). Boston, Massachusetts: Butterworth-Heinemann, Ltd., p. 15–136.

**Miller, R.D., and E. Dobrovolny** (1959) Surficial geology of Anchorage and vicinity, Alaska. Washington, DC: U.S. Geological Survey Bulletin 1093.

**Ovenshine, G.** (1970) Observations of iceberg rafting in Glacier Bay, Alaska, and the identification of ancient ice-rafted deposits. *Geological Society of America Bulletin*, **81**(3): 891–894.

**Powell, R.D., and E. Domack** (1995) Modern glaciomarine environments. In *Modern Glacial Environments: Processes, Dynamics, and Sediments* (J. Menzies, Ed.). Boston, Massachusetts: Butterworth-Heinemann, Ltd., p. 445–486.

**Repsold, H.** (1989) *Well Logging in Ground Water Development, International Contributions to Hydrology*. Hannover, Germany: Verlag Heinz Heise.

**Rust, B.R.** (1975) Fabric and structure in glaciofluvial gravels. In *Glaciofluvial and Glaciolacustrine Sedimentation* (A.V. Jopling and B.C. McDonald, Eds.). Tulsa, Oklahoma: Society of Economic Paleontologists and Mineralogists, Special Publication No. 23, p. 238–248.

**Reger, R.D., R.A. Combellick, and J. Brigham-Grette** (1995) Late-Wisconsinan events in the upper Cook Inlet region, southcentral Alaska. In *Short Notes on Alaskan Geology 1995* (R.A. Combellick and F. Tannian, Eds.). Fairbanks, Alaska: Alaska Division of Geological and Geophysical Surveys, p. 33–45.

**Schlumberger Educational Services** (1989) *Cased Hole Log Interpretation Principles/Applications*. Huston, Texas.

**Schmoll, H.R., and E. Dobrovolny** (1972) Generalized geologic map of Anchorage and vicinity, Alaska. Washington, DC: U.S. Geological Survey Miscellaneous Investigations Map I-787-A.

**Schmoll, H.R., B.J. Szabo, M. Rubin, and E. Dobrovolny** (1972) Radiometric dating of marine shells from the Bootlegger Cove Clay, Anchorage area, Alaska. *Geological Society of America Bulletin*, **83**(4): 1107–1114.

**Schmoll, H.R., L.A. Yehle, and E. Dobrovolny** (1996) Surficial geologic map of the Anchorage A-8 NE quadrangle, Alaska. Denver, Colorado: U.S. Geological Survey, Open-File Report 96-003.

**Smith, N.D.** (1970) The braided stream depositional environment: Comparison of the Platte River with Silurian clastic rocks, North-Central Appalachians. *Geological Society of America Bulletin*, **81**: 2993–3014.

**Smith, N.D.** (1985) Proglacial fluvial environment. In *Glacial Sedimentary Environments* (G.M. Ashley, J. Shaw, and N.D. Smith, Eds.). Tulsa, Oklahoma: Society of Economic Mineralogist and Petrologists, p. 85–134.

**Strasser, J.C., L.E. Hunter, A.J. Delaney, and D.E. Lawson** (1996) Reconnaissance ground-penetrating radar investigations of the subsurface geology, Fort Richardson, Alaska. U.S. Army Cold Regions Research and Engineering Laboratory. (CRREL Contract Report to U.S. Army, Alaska, Directorate of Public Works.)

**Thomas, G.S., and R.J. Connell** (1985) Iceberg drop, dump and grounding structures from Pleistocene glacio-lacustrine sediments, Scotland. *Journal of Sedimentary Petrology*, **55**(2): 243–249.

**USACE** (1996) Chemical data report: Groundwater study, Fall 1995, Fort Richardson, Alaska. Anchorage, Alaska: U.S. Army Engineer District, Alaska.

**USACE** (1997a) Operable Unit A, Informational Repository Administrative Record, Fort Richardson, Alaska. Anchorage, Alaska: U.S. Army Engineer District, Alaska.

**USACE** (1997b) Operable Unit C, Informational Repository Administrative Record, Fort Richardson,

Alaska. Anchorage, Alaska: U.S. Army Engineer District, Alaska.

**USACE** (1997c) Operable Unit D, Informational Repository Administrative Record, Fort Richardson, Alaska. Anchorage, Alaska: U.S. Army Engineer District, Alaska.

**Yehle, L.A., J.K. Odum, H.R. Schmoll, and L.L. Dearborn** (1986) Overview of the geology and geophysics of the Tikishla Park drill hole, USGS A-84-1, Anchorage, Alaska. Anchorage, Alaska: U.S. Geological Survey, Open-File Report 86-293.

**Yehle, L.A., and H.R. Schmoll** (1987a) Surficial geologic map of the Anchorage B-7 NE quadrangle, Alaska. Anchorage, Alaska: U.S. Geological Survey, Open-File Report 87-416.

**Yehle, L.A., and H.R. Schmoll** (1987b) Surficial geologic map of the Anchorage B-7 NW quadrangle, Alaska. Washington, DC: U.S. Geological Survey, Open-File Report 87-168.

**Yehle, L.A., and H.R. Schmoll** (1989) Surficial geologic map of the Anchorage B-7 SW quadrangle, Alaska. Anchorage, Alaska: U.S. Geological Survey, Open-File Report 89-318.

**Yehle, L.A., H.R. Schmoll, and E. Dobrovolny** (1990) Geologic map of the Anchorage B-8 SE and part of the Anchorage B-8 NE quadrangles, Alaska. Anchorage, Alaska: U.S. Geological Survey, Open-File Report 90-238.

**Yehle, L.A., H.R. Schmoll, and E. Dobrovolny** (1992) Surficial geologic map of the Anchorage A-8 SE quadrangle, Alaska. Anchorage, Alaska: U.S. Geological Survey, Open-File Report 92-350.

## GLOSSARY*

**Alluvial**: a general term (now considered obsolete) used to describe recent material deposited by a stream or running body of water, including floodplains, deltas, cones, and fans. However, it is commonly used on surficial geological maps to identify modern and ancient channel and floodplain deposits. *Glacioalluvial* is a specific usage that pertains to features or deposits associated with glacial streams.

**Aquifer**: a rock or sediment unit that is sufficiently permeable to conduct ground water and yield sufficient water for wells and springs. An aquifer is considered *confined* if it is bracketed by units with low permeability, limiting horizontal flow. Water in a confined aquifer is commonly under pressure, forming an *artesian aquifer*. An *unconfined aquifer* has no upper confining layer so that the upper limit of the water forms a free-water surface (i.e., pressure at the surface is equal to atmospheric pressure).

**Clast**: an individual grain of a sediment. In this report we use the term to describe grains larger than 1 cm in diameter.

**Clast support**: see sedimentary textures.

**Confined aquifer**: see aquifer.

**Confining layer**: a stratigraphic unit with a low permeability that retards ground water flow (i.e., aquitard).

**Couplet**: see sedimentary structures.

**Debris flow**: a mass of rock fragments, soil, mud, and water that flows under the influence of gravity.

**Diamicton**: a generic term used to describe unsorted or poorly sorted mixtures of clay, silt, sand, and gravel without implying a mode of origin. Often used synonymous with till in glacial studies.

**Discharge** (hydraulic use): the rate of fluid flow at a given time expressed as a volume per unit time.

**Distal** (in sedimentologic terms): refers to a depositional environment and associated deposits (fine grained) that are found removed from the sediment source, typically by distance.

**Drift**: a general term used to describe all rock material transported by a glacier and deposited by or from the ice, or by running water emanating from the glacier.

**Drumlin**: a smoothly rounded, elongate hill built or molded under a glacier composed of till or stratified glacial sediments, or both.

**Emergence**: a relative change in water level where areas formerly submerged by water become exposed to the air.

**End moraine**: see moraine.

**Estuarine**: adjective used to describe features associated with the environment where marine and fresh water mix, such as where a river valley or glacial trough (fjord) meets the sea.

**Facet**: a nearly plane surface on a rock or clast produced by abrasion (e.g., grinding action of a glacier).

---

*Terms are modified from Jackson (1997).

**Fissility**: see sedimentary structures.

**Floodplain**: the surface of relatively smooth land adjacent to a river channel that becomes submerged during a flood. The plain is composed of alluvium transported during floods and deposited during waning stages of flow.

**Fluvial**: adjective used to describe features or deposits that are related or produced by streams or stream processes.

**Glacioalluvial**: see alluvial.

**Glacial marine**: a general term used to describe the marine environment adjacent to a glacier and its associated deposits.

**Ground moraine**: see moraine.

**Holocene**: an epoch of the Quaternary period beginning at the end of the Pleistocene (10,000 radiocarbon years ago) and extending to present.

**Hummocky moraine**: see moraine.

**Hydrogeology**: of or pertaining to the science of subsurface water with consideration of geologic constraints.

**Isostasy**: the condition of equilibrium in units of the Earth's crust dependant on local thickness and density. *Isostatic adjustment* (or compensation) is a change in crust height in response to changes in mass to maintain this equilibrium.

**Lacustrine**: refers to the depositional environment of deposits associated with lakes.

**Late Wisconsinan**: the last phase of major glacial advance during the Pleistocene extending from about 35,000 to 10,000 radiocarbon year BP.

**Lateral moraine**: see moraine.

**Lithology**: a descriptive term referring to the physical rock or sediment character (adj.: lithologic).

**Lodgement**: the depositional process where sediment is "plastered" beneath a glacier onto bedrock or older sediments.

**Loess:** a widespread blanket deposit consisting predominantly of silt with subordinate quantities of clay to sand generally deposited as windblown dust during glacial periods.

**Matrix**: the finer-grained material enclosing, or filling the interstices between, larger grains of sediment.

**Matrix support**: see sedimentary textures.

**Marine transgression**: any change (sea level or land uplift) that causes an advance or enlargement of the sea that brings deep-water environments to areas formerly occupied by near-shore (shallow) environments, or that causes a shift in the boundary from non-marine to marine away from the center of the basin.

**Marine regression**: any change (sea level or land uplift) that causes a retreat or contraction of the sea from land that brings near-shore (shallow) environments to areas formerly occupied by deep-water environments, or that causes a shift in the boundary from marine to non-marine towards the center of the basin.

**Moraine**: a mound, ridge, or other accumulation of glacial sediment producing a variety of landforms. Includes:

*End-moraine*: a ridge or series of ridge segments deposited at the end (or terminus) of a glacier.

*Lateral moraine*: a ridge or ridge segments deposited at the side margin of a glacier (commonly form gently sloping, sharp crested ridges along the walls of valleys that glaciers formerly occupied).

*Ground moraine*: a general term used to describe the broad, commonly glacially streamlined surface produced under a glacier and left behind when the glacier retreated (composed of till of variable thickness with thin outwash gravel and lake deposits on the surface).

*Hummocky moraine*: an uneven, hilly topography formed along an active ice margin or around stagnant masses of ice.

**Mud**: an unconsolidated sediment consisting of clay, or silt, or both, with material of other dimensions (e.g., sand) mixed with water.

**Outburst flood**: a sudden release of water from a glacier or glacier-dammed lake resulting in a catastrophic flood.

**Outwash**: refers to the sediment and water discharged from a glacier. Deposition of the sediments produce broad, gently sloping sheets (*outwash aprons, outwash plains*) or fan shaped features (*outwash fans*).

**Overconsolidated**: a condition where consolidation is greater than that normal for the existing overburden. Used synonymously with *overcompacted* in this report.

**Perched ground water**: unconfined ground water located above a unit of low permeability that is separated from the underlying ground water by an unsaturated zone.

**Pebbly mud:** a sediment with scattered pebbles floating in an abundant muddy matrix forming a clast-poor diamicton.

**Poorly sorted**: see sedimentary textures.

**Proximal (in sedimentologic terms)**: refers to a depositional environment and associated deposits (coarse grained) that are found adjacent to or near the sediment source.

**Quaternary**: a period in geological time extending from the end of the Tertiary (2–3 million years ago) to present. This roughly represents the time when large ice sheets advanced and retreated over large segments of the Northern Hemisphere.

**Saprolite**: a soft, earthy, typically clay-rich and thoroughly decomposed rock formed by chemical weathering of a parent rock.

**Sedimentary structures**: structures in a rock or sediment formed during deposition or shortly thereafter because of sedimentary processes.

- *Beds*: well defined sedimentary units greater than 1 cm thick; their upper surface is called bedding or bedding surface.
- *Couplets*: genetically related paired sedimentary laminations, generally occurring in repeating series (e.g., varves).
- *Cross bedding*: layers or laminae deposited at an angle relative to the main depositional surface.
- *Cut and fill*: a sedimentary structure consisting of a small erosional channel that has been subsequently refilled; often identifiable by changes in sediment texture between the sediment fill and surrounding sediment.
- *Fissility*: a general term used to describe the property of some materials to split along thin, closely spaced layers.
- *Grading*: the gradual change in particle size within a stratification unit; *normal grading* refers to the gradual decrease in particle size from the sole to top of a unit; *inverse grading* is the gradual increase in particle size above the base.
- *Laminae*: well defined sedimentary units less than 1 cm thick.
- *Massive*: a descriptive term for thin-bedded sediments where individual beds (or strata) are generally without internal structure.
- *Unconformity*: a depositional surface upon which younger sediments overlie older sediments, but are not in stratigraphic succession. Depositional interruption (as used in report) often represents erosion and truncation of lower sedimentary layers.

**Sedimentary textures**: small-scale features in a sediment or sedimentary rock caused by changes in shape, size, orientation, and packing of particles.

- *Open framework*: a specific term used to describe gravels that lack a matrix and are clast-supported; commonly have high porosity and permeability.
- *Support*: a general term used to describe the three-dimensional relationship of larger particles within a sediment; *clast-supported* refers to a sediment where the larger particles (granules, pebbles, cobbles, etc.) are in grain-to-grain contact within three-dimensional space; a *matrix-supported* fabric occurs where these larger particles are suspended within a sand or mud matrix and do not experience grain-to-grain contacts.
- *Sorting*: refers to the particle size distribution of a sediment relative to a mean size. Poorly sorted sediment are characterized by a widely distributed particle size

distribution (generally synonymous with the civil engineering term well graded); well-sorted sediments are characterized by a narrowly distributed particle size range where particles are roughly the same size (generally synonymous with poorly graded).

**Stratigraphic architecture**: refers to the three-dimensional distribution and relationships among deposits below the ground surface.

**Stratigraphy**: the arrangement of depositional units or deposits below the ground surface and their chronological order of sequence. *Stratification* is the structure produced by the deposition of sediments in strata (layers).

**Striation**: one or multiple scratches inscribed on a rock surface by a geologic agent (e.g., glacier).

**Submergence**: a relative change in water level where areas formerly exposed to the air become submerged by water.

**Surficial geology**: covers a broad range of study of unconsolidated deposits lying on bedrock at or near the surface of the Earth.

**Tertiary**: the first period of the Cenozoic era extending from 65 million to 2–3 million years ago. It is divided into the Paleocene, Eocene, Oligocene, Miocene, and Pliocene epochs.

**Thixitropic**: the property of a fine-grained sediment to weaken when shaken or increase strength upon standing.

**Till**: a sedimentary deposit typically consisting of poorly sorted and poorly stratified material laid down beneath a glacier. Tills generally have a high percentage of fine-grained silt or clay, which gives them a low permeability to water flow.

**Well sorted**: see sedimentary textures

**Unconfined aquifer**: see aquifer.

**Unconformity**: see sedimentary structures.

# REPORT DOCUMENTATION PAGE

*Form Approved*
*OMB No. 0704-0188*



| 1. REPORT DATE *(DD-MM-YY)* | 2. REPORT TYPE | 3. DATES COVERED *(From - To)* |
|---|---|---|
| September 2000 | Technical Report | |

**4. TITLE AND SUBTITLE**

Geological Investigations and Hydrogeological Model of Fort Richardson, Alaska

**5a. CONTRACT NUMBER**

**5b. GRANT NUMBER**

**5c. PROGRAM ELEMENT NUMBER**

**6. AUTHOR(S)**

Lewis E. Hunter, Daniel E. Lawson, Susan R. Bigl, Beth N. Astley, Colby F. Snyder, and Frank E. Perron, Jr.

**5d. PROJECT NUMBER**

**5e. TASK NUMBER**

**5f. WORK UNIT NUMBER**

**7. PERFORMING ORGANIZATION NAME(S) AND ADDRESS(ES)**

U.S. Army Engineer Research and Development Center
Cold Regions Research and Engineering Laboratory
72 Lyme Road
Hanover, New Hampshire 03755-1290

**8. PERFORMING ORGANIZATION REPORT NUMBER**

ERDC/CRREL TR-00-18

**9. SPONSORING/MONITORING AGENCY NAME(S) AND ADDRESS(ES)**

U.S. Army Alaska
Fort Richardson, Alaska

**10. SPONSOR / MONITOR'S ACRONYM(S)**

**11. SPONSOR / MONITOR'S REPORT NUMBER(S)**

**12. DISTRIBUTION / AVAILABILITY STATEMENT**

Approved for public release; distribution is unlimited.

Available from NTIS, Springfield, Virginia 22161.

**13. SUPPLEMENTARY NOTES**

**14. ABSTRACT**

The glacial stratigraphy of Fort Richardson reflects deposition in glacial and glacial–marine environments during multiple retreat phases following the last glacial maximum. A preliminary model relied heavily on the glacial history of the region, mapping by the U.S. Geological Survey, and limited borehole logs. This report expands on that model and describes new subsurface data obtained from field observations and descriptions of stratigraphic exposures and core samples from 28 new boreholes between 1997 and 1998. Geophysical techniques were applied to seven of the new boreholes and 25 existing monitoring wells, augmenting surface techniques (ground resistivity and ground penetrating radar). Beneath the cantonment is a thick unconfined aquifer, apparently deposited as a large alluvial fan (Mountain View fan), that overlies a fine-grained confining layer composed of mud and diamicton. The diamicton is a subglacial lodgement deposit bracketed by stratified debris flow deposits, being thickest to the southeast, dipping and thinning to the north and west where deposits of the Mountain View fan truncate the confining horizon, providing potential hydraulic communication between the upper (unconfined) and lower (confined) aquifers. A second mud–diamicton horizon forms a deeper (38–66 m depth) confining layer and also appears to extend across the cantonment. Between the upper and lower confining diamicton horizons are coarse, sandy gravels that make up a confined aquifer. Ground water in the unconfined aquifer flows generally to the northwest, presumably recharged by Ship Creek. When ground water levels are low (i.e., winter), flow is locally diverted by irregularities in the surface of the upper confining layer. When recharge is high, regional flow is unaffected by these irregularities. Ground water in the confined aquifer also flows to the northwest, following the slope of the potentiometric surface.

**15. SUBJECT TERMS**

Anchorage, Alaska; Elmendorf Moraine; Fort Richardson; Geophysics; Glacial stratigraphy; Hydrogeology; Quarternary geology

| 16. SECURITY CLASSIFICATION OF: | | | 17. LIMITATION OF ABSTRACT | 18. NUMBER OF PAGES | 19a. NAME OF RESPONSIBLE PERSON |
|---|---|---|---|---|---|
| a. REPORT | b. ABSTRACT | c. THIS PAGE | | | 19b. TELEPHONE NUMBER *(include area code)* |
| U | U | U | U | 58 | |